MASTER

A Cellular Neural Network : the design of a Full-Range Cellular Neural Network and a method to find the Basin of Attraction in CNN's

Wilmans, R.T.

Award date:
1997

A Cellular Neural Network

The design of a Full-Range Cellular Neural Network and a method to find the Basin of Attraction in CNN's.

Author: R.T. Wilmans

Student at: Eindhoven University of Technology

ID-number: 365542

Coaches: J.A. Hegt and D.M.W. Leenaerts

Place: Eindhoven University of Technology,
Faculty of Electrical Engineering,
Systems for Electronic Signal processing

Date: 19-8-1997

Summary

This report is about the hardware design of a Full-range Cellular Neural Network (FR-CNN). Also in this report a method is suggested to find the boundaries of the basins of attraction (BOA) for 2-cell CNN's.

A FR-CNN is a neural network consisting of identical neurons or cells with space-invariant templates, modified in such way that it operates conform the Full range model. This model has the advantage that the state of a cell is confined between certain values, independent of the template parameters through which neighbouring cells affect the state of the cell.

A circuit is suggested to implement a cell of a FR-CNN. It is shown that the suggested circuit does not function properly and a modification to this circuit is made after which a well-functioning cell circuit is obtained.

The boundaries of the basins of attraction of CNN's (not necessarily FR-CNN's) are the borders that separate regions in state space. These regions (basins of attraction) are the areas where a CNN converges to a specific equilibrium point.

To find the BOA in a 2-cell CNN a certain Lyapunov energy function is more closely investigated and (with some restrictions) a force is introduced. Finally the BOA is found by solving the differential equations, describing the cells' behaviour.

Contents

1 Introduction

After the rebirth of the interest for artificial Neural Networks in 1982 [1], many different implementations for this concept have been developed. The differences between these implementations affect the overall characteristics of the network and thus the applicability for a certain purpose like, for example, real time image processing. Here, an important feature of neural networks is touched upon; these circuits can operate very fast since the 'signal processing' is done simultaneously in parallel neurons, rather than in sequential time steps.

The major disadvantage of most neural network implementations however is the number of interconnections between neurons. In order to reduce the number of interconnections but keep the advantages of parallel processing, Chua and Yang proposed a so-called Cellular Neural Network (CNN) in 1988 [2] where neurons were only connected to other neurons within a certain neighbourhood.

In 1992, Rodriguez-Vázquez proposed a modified model for neurons; the so-called Full Range (FR) model and an implementation for a CNN in the current domain based on this FR-model. [3]. In 1996 P. Bruin suggested an implementation for a FR-CNN in the voltage domain. However, after realisation of the implementation, it was found to display instabilities.

In this report the properties of the FR-model and Rodriguez-Vázquez' implementation are investigated and a different implementation for a CNN based on the FR-model is suggested.

Every neuron in a cellular neural network can be described by a certain state-equation. If this network consists of two interconnected cells, the behaviour that is displayed by those cells can be plotted in a so-called state space. It is interesting to be able to 'predict' to what final state the CNN will converge. For this, the state-space will be partitioned into 'basins of attraction', separated by certain boundaries.

In this report a method to find the boundaries of the basins of attraction is proposed.

2 A Cellular Neural Network

A Cellular Neural Network (CNN) is an artificial neural network consisting of separate neurons or cells. It has several properties that may be advantageous compared to other neural networks. The dynamic range of a CNN for example is bounded. Also a CNN can easily be extended without having to re-adjust the entire network because a cell is not connected to every other cell in the network but rather to cells within a certain neighbourhood. Albeit its cellular structure it still displays the complex dynamic behaviour as seen with other neural networks. Due to this complex behaviour it can be used in image processing (e.g. noise-removal, connected component detection (CCD), 'thinning' etc.) It can also be used to simulate certain equations or be used as an associative memory.

Another advantage is that although the factor with which the output of a cell affects the behaviour of other cells (template parameter) may be different for spatially different neighbouring cells, the template thus formed is translational invariant ('cloning templates').

As stated above, these cells can interact with other cells within a certain neighbourhood. A rectangular two-dimensional CNN consisting of 16 cells where every cell interacts with only its directly neighbouring cells would look like the circuit shown in Figure 1.

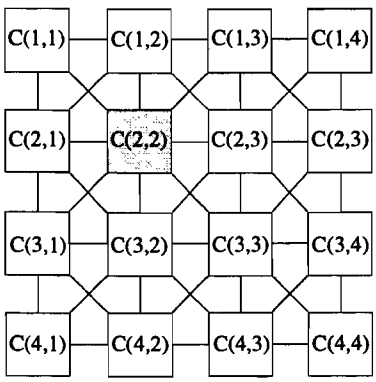

Figure 1 A CNN (4x4) with r=1

If C(i,j) is the cell on the i^{th} row and j^{th} column then cell C(2,2) is connected to C(1,1), C(1,2), C(1,3), C(2,1), C(2,2), C(2,3), C(3,1), C(3,2) and C(3,3).

A so called r-neighbourhood is defined as:

$$N_r(i,j) = \left\{ C(k,l) \middle| \max\left[|k-i|,|l-j|\right] \le r,\ 1 \le k \le M; 1 \le l \le N \right\} \tag{1}$$

with M and N the number of rows and columns respectively and 'r' a positive integer.

It's easily seen that Figure 1 depicts a r-neighbourhood with r=1. For technical implementation intercell connectivity with r=1 is the easiest to realise and exhibits a less complex behaviour than CNN's with r≥2.

The equation with which the time-dependent dynamics of a cell in a CNN can be described was proposed by Chua and Yang [2] and is given by:

$$C\frac{dV_{xij}(t)}{dt} = -\frac{V_{xij}(t)}{R_x} + \sum_{C(k,l)\in N_r(i,j)} A(i,j;k,l)\cdot V_{ykl}(t) + \sum_{C(k,l)\in N_r(i,j)} B(i,j;k,l)\cdot V_{ukl}(t) + I \tag{2}$$

with $1 \le i \le M$, $1 \le j \le N$. It is assumed that $|V_{xij}(0)| \le 1$ and $|V_{uij}| \le 1$, $C > 0$ and $R_x > 0$. The time-dependent variable $V_{xij}(t)$ is called the 'state' of the cell and can be represented by the voltage across a (state-) capacitor.

Assuming an r=1 neighbourhood in a two-dimensional CNN, there are nine terms in equation (1) that affect the state of the cell $V_{xij}(t)$ by means of the output voltages $V_{ykl}(t)$ of neighbouring cells: $A(i,j;k,l)\cdot V_{ykl}(t)$

Also there are nine terms depending on the input voltages (V_{ukl}) of the neighbouring cells: $B(i,j;k,l)\cdot V_{ukl}$

Since the terms that affect that voltage across a capacitor are currents, use can be made of voltage controlled current sources (VCCS) to account for these terms.

If

$$I_{xy}(i,j;k,l) = A(i,j;k,l)\cdot V_{ykl}(t)$$

and

$$I_{xu}(i,j;k,l) = B(i,j;k,l) \cdot V_{ukl}$$

then the terms that affect the state of cell (i,j) due to input- and output voltages of neighbouring cells (V_{ukl} and V_{ykl} respectively) are accounted for.

The constant input voltage V_{uij} of cell (i,j) is set by a voltage source E_{uij} and the constant I may be implemented using a constant current source with magnitude I. The term $-\frac{V_{xij}(t)}{R_x}$ can be obtained by connecting a resistor R_x in parallel with the state capacitor.

The cell circuit as proposed by Chua and Yang [2] is shown in Figure 2.

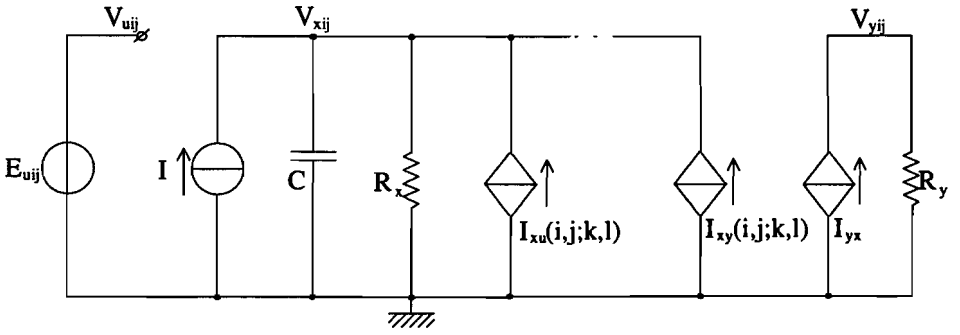

Figure 2 The proposed cell circuit

Since the network is two-dimensional (or multi-dimensional in general), 'A(i,j;k,l)' and 'B(i,j;k,l)' can be represented by matrices and are called feedback- and control operator respectively for obvious reasons. These matrices are the same for every cell in the network (spatially invariant) so only two matrices need to be given (for the feedback- and control operator respectively). For this reason the templates thus formed are also called 'cloning templates'.

The aforementioned VCCS's are linear devices except for the current source that drives the output voltage V_{yij} via the output resistor R_y. This is a non-linear device and has a transfer function:

$$I_{yx} = \frac{f(V_{xij})}{R_y}$$

$$\text{with} f(V_{xij}) = \frac{1}{2}\left[|V_{xij}+1| - |V_{xij}-1|\right]$$

As is shown by Chua and Yang [2] the steady state outputs of the CNN are constants and are either ±1, regardless of the exact value of the initial conditions- if it is assumed that :

$$\left.\begin{array}{l} |V_{xij}(0)| \le 1 \\ |V_{uij}| \le 1 \end{array}\right\} 1 \le i \le M \quad 1 \le j \le N \qquad \underbrace{A(i,j;k,l) = A(k,l;i,j)}_{1\le i,k\le M;\,1\le j,l\le N} \qquad A(i,j;i,j) \ge \frac{1}{R_x} \tag{3}$$

The state equation (2) can be rewritten to provide a better insight into the behaviour of the cell due to the 'actions' of neighbouring cells.

$$C\frac{dV_{xij}(t)}{dt} = \underbrace{\sum_{\substack{C(k,l)\in N_r(i,j) \\ C(k,l)\neq C(i,j)}} \left\{A(i,j;k,l)\cdot V_{ykl}(t) + B(i,j;k,l)\cdot V_{ukl}\right\} +}_{g(t)} \tag{4}$$

$$\underbrace{-\frac{V_{xij}(t)}{R_x} + A(i,j;i,j)\cdot V_{yij}(t) + B(i,j;i,j)\cdot V_{uij} + I}_{h(V_{xij}(t))}$$

$$C\frac{dV_{xij}(t)}{dt} = g(t) + h(V_{xij}(t)) \tag{5}$$

Thus g(t) represents the behaviour of the cell caused by other cells whereas h(t) represents the cell's behaviour if there were no neighbouring cells. The phase diagram can be plotted and if the constant current I is assumed to be zero the phase diagram will look like Figure 3.

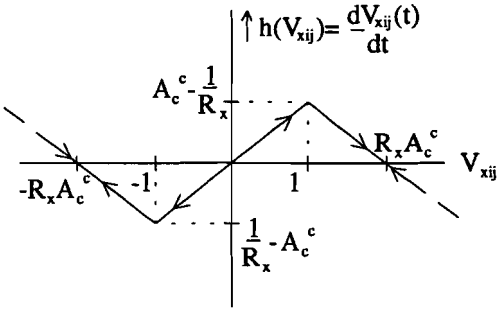

Figure 3 The behaviour of the cell

Since the unit of g(t) and h(t) is Ampere the actions of neighbouring cells acting via g(t) can be represented by a current source with a magnitude equal to g(t). Ignoring the influence of g(t) (by assuming there are no neighbouring cells) shows that $\frac{dV_{xij}(t)}{dt}$ is negative if $-R_xA_c^c < V_{xij}(t) < 0$ and $V_{xij}(t)$ will become more negative. If $V_{xij}(t) < -R_xA_c^c$ then $\frac{dV_{xij}(t)}{dt}$ becomes positive and $V_{xij}(t)$ will increase and tend towards $-R_xA_c^c$. From this it can be seen that if $V_{xij}(t)<0$, $V_{xij}(t)$ will eventually remain at $-R_xA_c^c$ which is called a stable equilibrium point. A slight deviation from this point will result in such a $\frac{dV_{xij}(t)}{dt}$ that $V_{xij}(t)$ will always return to the stable equilibrium point.

Likewise it can be concluded that if $V_{xij}(t)>0$, $V_{xij}(t)$ will tend towards $R_xA_c^c$, which is another (stable) equilibrium point. If $V_{xij}(t)=0$ then $V_{xij}(t)$ neither becomes positive nor negative. A small deviation from this point however does not cause $V_{xij}(t)$ to return to $V_{xij}(t)=0$. Thus $V_{xij}(t)=0$ is said to be an instable equilibrium point.

If g(t) is a non-zero constant then $\frac{dV_{xij}(t)}{dt}$ is no longer equal to $-h(V_{xij})$ but equal to $-h(V_{xij})+g(t)$. Therefore $\frac{dV_{xij}(t)}{dt}$ will be equal to a vertically shifted (by g(t)) version of Figure 3. However, in general the state of neighbouring cells may vary as functions of time and so g(t) will not be a constant. Moreover, cell (i,j) itself may cause g(t) to change due to the dynamic interactions between cells. This will result in a (vertical) shifted version of Figure 3 with the shift being a certain complex function of time.

3 The Full Range model

In 1992, Rodriguez-Vázquez introduced a new model to overcome several drawbacks of the implementation as proposed by Chua and Yang [2]. One of these drawbacks is that the primary output of image sensor devices is a current and therefore the interface design for image processing tasks will be complicated [3]. An other drawback is that the state variable is bounded, but can vary in a large range, depending on the templates (certain values for feedback- and control operators). This may complicate VLSI implementation, whereas the state variable in Rodriguez-Vázquez' Full Range model is always comprised between -1 and +1 (normalised) independent of the templates.

With the Full Range model, the state-equation is given by:

$$\tau \frac{dx^c(t)}{dt} = g\left[x^c(t)\right] + \sum_{d \in N_r(c)} \left\{ A_d{}^c y^d(t) + B_d{}^c u^d \right\} + D^c$$

$$\text{with} \quad g\left(x^c\right) = \lim_{m \to \infty} \begin{cases} -m\left(x^c + 1\right) + 1 & x^c < 1 \\ -x^c & \text{otherwise} \\ -m\left(x^c - 1\right) - 1 & x^c > 1 \end{cases} \qquad (6)$$

$$\text{and} \quad y^c = f\left(x^c(t)\right)$$

where x^c is the state variable of cell 'c' according to $V_{xij}(t)$ with Chua and Yang, D^c is the offset parameter (according to the term I), $A_d{}^c$ and $B_d{}^c$ are the feedback- and control operator (according to $R_x \cdot A(i,j;k,l)$ and $R_x \cdot B(i,j;k,l)$ respectively), y^d denotes the output variable of cell 'd' ($V_{ykl}(t)$) and u^d the input variable of cell 'd' (corresponding with V_{ukl}).

If m=1, this model reduces to the original Chua-Yang model. Here too, the state-equation can be rewritten to show the effect of other cells on the state of cell 'c'. The term independent of the state of cell 'c' can be written as:

$$I' = D^c + B_c{}^c u^c + \sum_{\substack{d \in N_r(c) \\ d \neq c}} \left\{ A_d{}^c y^d + B_d{}^c u^d \right\} \qquad (7)$$

If the term I' is assumed to be zero (which is equal to stating that there is neither an offset nor a constant input and that there are no neighbouring cells) then the state equation reduces to: $\tau \frac{dx^c}{dt} = g(x^c) + A_c{}^c x^c$ and is illustrated in Figure 4.

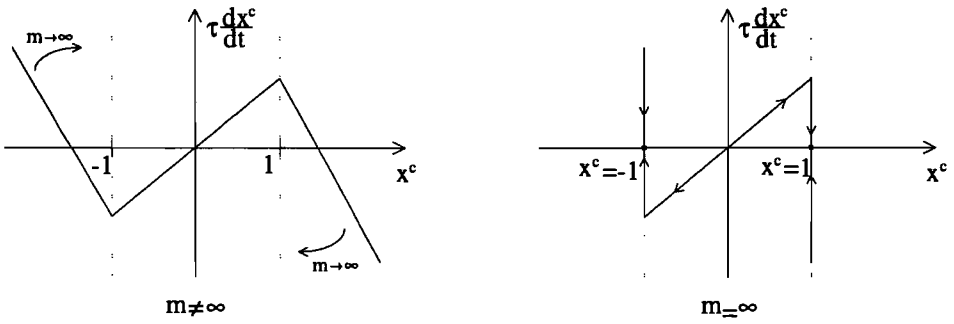

Figure 4 Phase-diagram of the full-range cell behaviour

Like was the case in the Chua-Yang model, a non-zero factor I' results in a vertical shift of the characteristics shown in Figure 4. Note that here too, the vertical shift depends on the outputs of neighbouring cells and thus varies as a function of time. As can be seen in Figure 4, the state variable cannot be larger than ±1 if m=∞.

Assuming I'=0 and m=∞, the slope of the inner region ($|x^c| < 1$) is $A_c{}^c$-1. If furthermore $A_c{}^c$>1 then $\tau \frac{dx^c}{dt}$ is positive for positive values of x^c and negative for negative values of x^c. The state can be said to be driven towards the outer regions. However, should the state come into one of the outer regions, it would be 'pushed back' infinitely fast towards the inner region due to the factor 'm' which is infinite. For the left outer region (or: left clipping region) it can be found:

$$\tau \dot{x} = -m(x+1) + 1 + A_c{}^c x + Z \tag{8}$$

with Z the effect caused by other cells, the input of the cell and D^c and assumed to be a constant in this equation. The solution is found to be:

$$x = \frac{1-m+Z}{m-A_c{}^c} + Be^{-\frac{m-A_c{}^c}{\tau}t} = x^c \tag{9}$$

$$\text{and } \lim_{m\to\infty} x^c = -1$$

with B a constant. So when the system is in the outer left region, it will converge to the stable state in the left clipping region. For the dynamic (inner) region it is found that:

$$\tau \dot{x} = Z + A_c{}^c x - x \tag{10}$$

with Z a 'constant' term to take into account the neighbouring cells, the input of the cell and the term D^c. Solving this equation leads to an expression for the state:

$$x = -\frac{Z}{A_c{}^c - 1} - Be^{\frac{A_c{}^c - 1}{\tau} t} \tag{11}$$

again with B a constant. Here the actions of the cell depend on the initial conditions. Assume that at time t=0, the influence Z causes the function to look like Figure 5, then Z is negative. If the state is at point 'P' (x^c=0) at time t=0 then for B we can find: $B = \frac{Z}{A_c{}^c - 1}$. So: $\dot{x} = \frac{A_c{}^c - 1}{\tau} \cdot B \cdot e^{\frac{A_c{}^c - 1}{\tau} t} = \frac{Z}{\tau} \cdot e^{\frac{A_c{}^c - 1}{\tau} t}$ which is negative since Z is negative and the state will move towards the left clipping region. For positive Z it can be found that the state goes towards the right-hand clipping region, for which there's one stable state as can be proven the same way as was done for the left-hand clipping region.

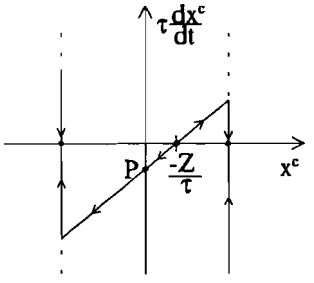

Figure 5 The influence of 'Z' on the phase diagram

A continuous-time CNN conceptual cell diagram for the **Chua-Yang model** is shown in Figure 6. The diagram of the FR-model according to the theory of **Rodriguez-Vázquez** is shown in Figure 13. Rodriguez-Vázquez states that 'for the full range model the non-linear block is eliminated and the function g(.) realised exploiting the output saturation of the integrator block'. As can be seen, the state x^c of the cell is a saturated function and will not become larger than unity.

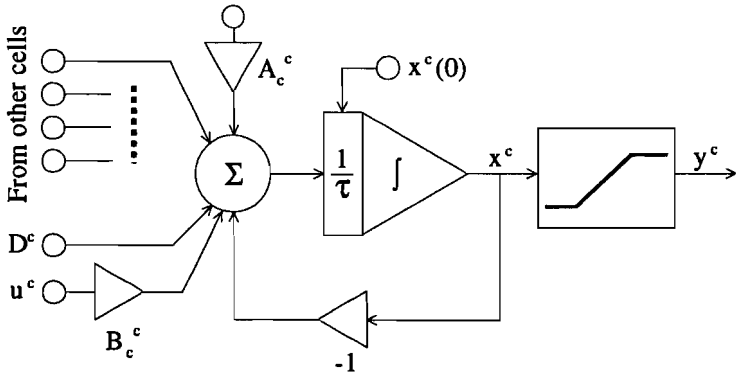

Figure 6 Conceptual cell diagram corresponding to the Chua-Yang model

However, the actual implementation given by Rodriguez-Vázquez to implement the FR-model does not correspond to the diagram as shown in Figure 13.

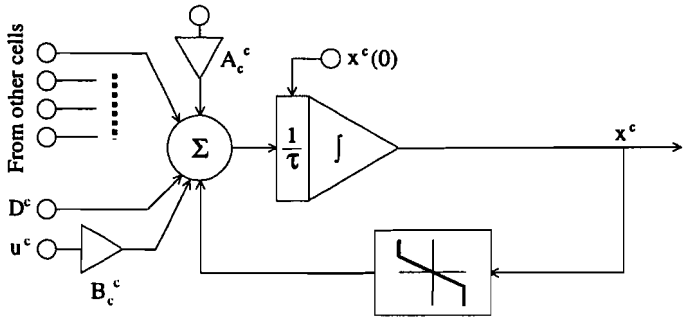

Figure 7 Conceptual diagram of the full range model given by Rodriguez-Vázquez

3.1 Implementation in current-domain

To show that the implementation as suggested by Rodriguez-Vázquez does not realise an FR-CNN, this circuit must be more closely looked at. The implementation in the current-domain makes use of transconductors (See Figure 8)

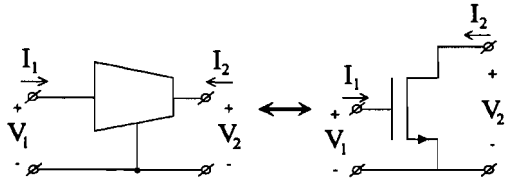

Figure 8 A transconductor and a single-MOST implementation

For a non-inverting current amplifier with the saturation non-linearity, Rodriguez-Vázquez suggests the circuit shown in Figure 9.

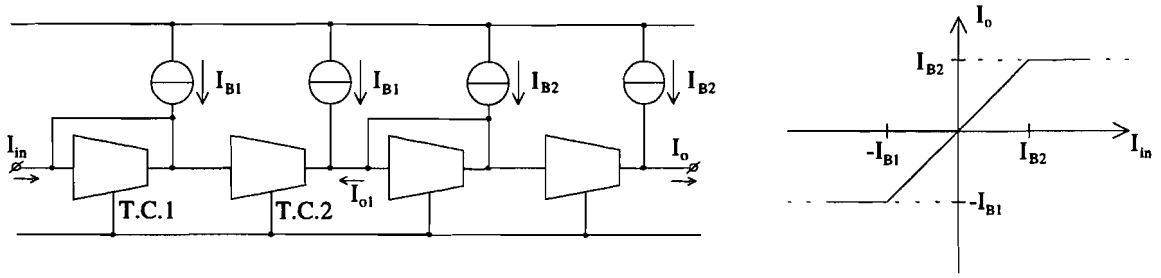

Figure 9 Non-inverting current amplifier

If $I_{B1}<I_{in}<I_{B2}$ and assuming the input current of transconductor 2 (T.C.2) is zero, the output current of T.C.1 is equal to $I_{in}+I_{B1}$. Therefore $I_2\big|_{T.C.2} = I_{in} + I_{B1}$ and $I_{o1}=I_{in}$. If $I_{in}>I_{B2}$ then $I_2\big|_{T.C.1} = I_{in} + I_{B1}$ but $I_{o1}=I_{B2}$ since the output current of a transconductor cannot be negative if the transconductors are realised using a MOST an assuming it operates in normal modes. Likewise, I_{in} cannot be more negative than $(-I_{B1})$. Thus the saturation non-linearity is achieved.

To obtain an integrator, a capacitor is added as shown in Figure 10.

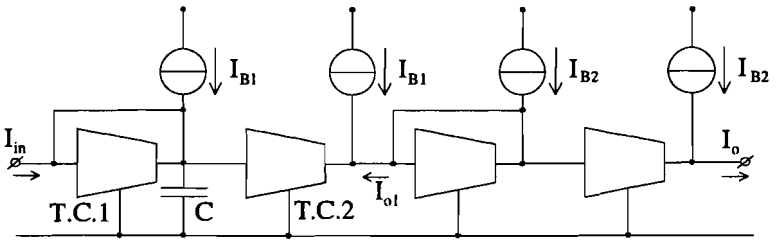

Figure 10 Current mode integrator

If $I_{in}>I_{B2}$ then eventually $I_2\big|_{T.C.1} = I_{in} + I_{B1}$ and $I_{o1}=I_{B2}$. However, if $I_{in}<-I_{B1}$ (which is possible since the capacitor can be discharged) then $I_o=I_{B1}$. So the output current is clipped, but the capacitor is discharged. If (due to other cells) the current I_{in} changes sign and becomes larger than or equal to $(-I_{B1})$ the capacitor first has to be recharged before the output current starts following the input current again. It is as if the state of the cell is driven into the clipping-region. To verify this assumption, the differential equation can be written down, assuming $I_{in}>I_{B2}$ (see Figure 11)

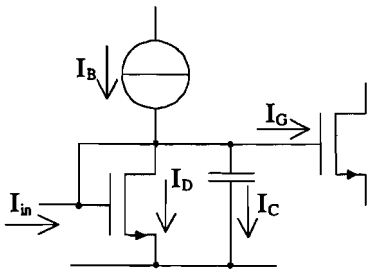

Figure 11 Currents through the components

Since V_{GD}=0 the NMOST parallel to the capacitor is always saturated and assuming I_G=0 we can find:

$$\begin{aligned} I_{in} + I_B &= I_d + I_c \\ I_{in} + I_B &= K\left(V_c - V_t\right)^2 + C\frac{dV_c}{dt} \end{aligned} \tag{12}$$

The steady state solution for V_c can be found by stating that $\frac{dV_c(t)}{dt} = 0$.

Then it is found that:

$$\lim_{t\to\infty} V_c = \sqrt{\frac{I_{in} + I_B}{K}} + V_t \tag{13}$$

Thus it can be seen that if I_{in} becomes a very large constant current, the capacitor will be charged accordingly. The output current however is 'clipped' and will only start to change if the capacitor is discharged enough, meaning that a time-delay will occur depending on the charge that was stored on the capacitor while the output current of the current mode integrator was clipped. See Figure 12.

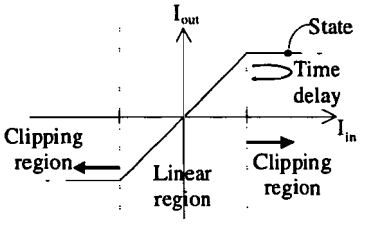

Figure 12 State of the cell vs. the output current

This is a behaviour that differs from what can be concluded from the theory of the FR-CNN. The system can be said to be driven into the clipping region and thus the circuit

proposed by Rodriguez-Vázquez does not implement a FR-CNN. (See equation (6) and Figure 4). This also becomes clear if the conceptual diagram of the full range model given by Rodriguez-Vázquez (Figure 7) is compared with the conceptual diagram of the implementation. See Figure 13.

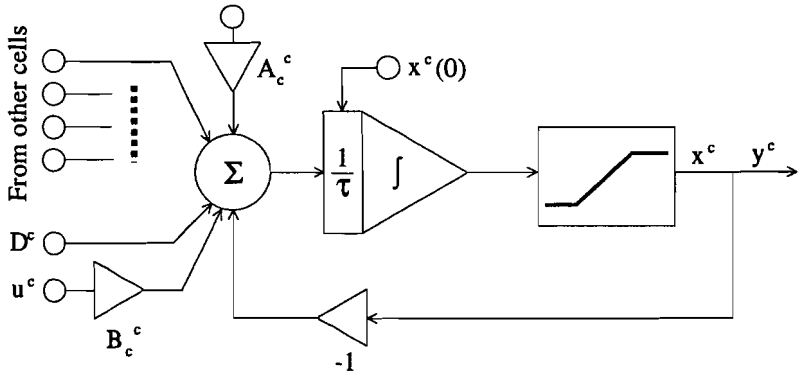

Figure 13 Conceptual diagram of implementation given by Rodriguez-Vázquez

3.2 The implementation of P. Bruin

The implementation of P. Bruin [4](1996) uses a three-transistor multiplier to establish the (programmable) feedback- and control operators, a current mirror and an active integrator using an opamp. As was shown by J. van Engelen [5], two-quadrant multipliers may be used to establish the feedback- and control operators if the template parameters are adjusted. The three-transistor multipliers that were used by P. Bruin are two-quadrant multipliers.

In this circuit the state-conditions are represented by a voltage, see Figure 14. The opamp is used to keep the node connected to the current mirror at virtual ground so the transistors of the current mirror and multiplier remain biased correctly. In order to do the 'clipping' - that is, to clamp the state voltage at a certain level (make m=∞), the voltage across the capacitor is compared to a pre-defined voltage. If the upper or lower clipping voltage is reached, the according comparator-output goes down to ground potential (or negative voltage supply) and shuts off the current supply by turning off the transistors between the multipliers and current mirrors. This way, no current is supplied to the (active) integrator, thereby causing the output voltage (which is equal to the state voltage) to saturate. Note that 19 multipliers are connected in parallel.

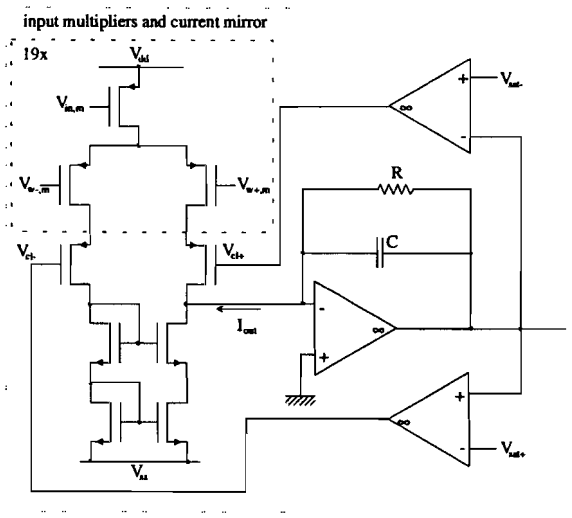

Figure 14 Circuit as proposed by P. Bruin

There are several remarks that can be made. First, the feedback loop to control the current that (dis-)charges the integrator is rather large. The current is cut off via a current mirror, an active integrator (which has time constants of its own due to the opamp) and a comparator (which introduces other time constants). This may result in a slow system, a phase-response that is incorrect etc. Furthermore in general, op-amps without (negative) feedback may result in instable circuits.

The circuit of P. Bruin is not driven further into the clipping region since the current that (dis-)charges the capacitor of the integrator is cut off. Hence the implementation of P. Bruin at system-level corresponds to the theory of Rodriguez-Vázquez as can be seen from the conceptual diagram in Figure 13, and does not correspond to the implementation given by Rodriguez-Vázquez.

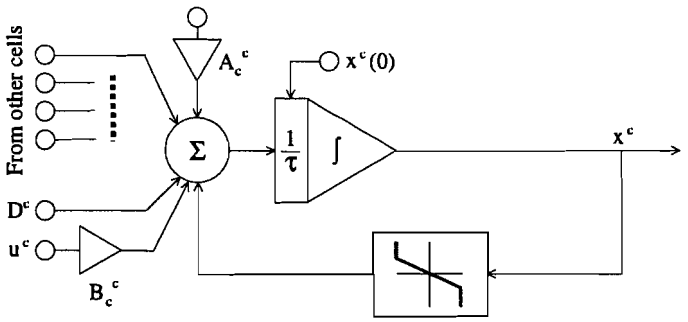

Figure 15 Diagram of circuit given by P. Bruin

3.3 Verification of the FR-formula

To verify whether an implementation that is searched for should be based on the FR-formula (as is P. Bruin's), a Matlab-program is written. This program simulates an array of cells (8x8) and uses an algorithm that does not allow for the state to be driven further into the clipping region according to the FR-formula (6). The output of the program shows the output of each individual cell plotted against time. The state is clipped at ±1. The cells are given only an initial value, then the relaxation process is not interfered with until the end of the simulation. See Figure 16.

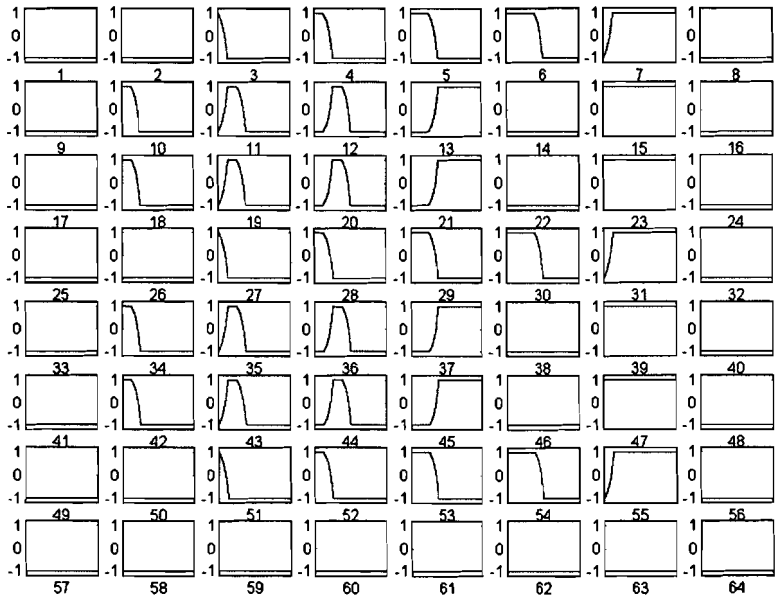

Figure 16 Output of cells shown graphically

As can be seen from these results, the behaviour that is displayed when an algorithm is used based on the formulas seems to be correct if so called connected component detection (CCD) is applied. See [5],[4] and [6]. Connected component detection is

usually applied to an image where every pixel has a binary value. With CCD the image is observed in a certain direction (from right to left for example). Every change in the binary value of the subsequent pixels is represented with a change in value of only one pixel in the resulting image. If a row of pixels in an image is depicted with: (○ ○ ○ ● ○ ● ● ● ○ ○) then the same row in the resulting image will be: (○ ○ ○ ○ ○ ○ ● ○ ● ○) if the row was observed from right to left.

In the Matlab program that was written, a few assumptions were made. As can be seen from the formulas, a cell's output/state influences its state via two feedback loops; the function $g(x^c)$ (See (6)) and the self-feedback parameter A_c^c. For normal Chua-Yang operation: $g(x^c)=-x^c$. These two feedback loops can be combined and a new feedback-loop $g'(x^c)$ is obtained. So:

$$\tau \frac{dx^c}{dt} = g[x^c(t)] + D^c + \sum_{d\in N_r(c)} \{A_d^c y^d(t) + B_d^c u^d\} = g'[x^c(t)] + I$$

$$\text{with} \quad I = D^c + \sum_{\substack{d\in N_r(c) \\ d\neq c}} \{A_d^c y^d(t) + B_d^c u^d\} + B_c^c u^c \qquad (14)$$

$$\text{and} \quad g'[x^c(t)] = g[x^c(t)] + A_c^c y^c(t)$$

$$y^c(t) = \tfrac{1}{2}\left(|x^c(t)+1| - |x^c(t)-1|\right) \qquad \text{for Chua - Yang Operation}$$

$$y^c(t) = x^c(t) \qquad \text{for FR - CNN's}$$

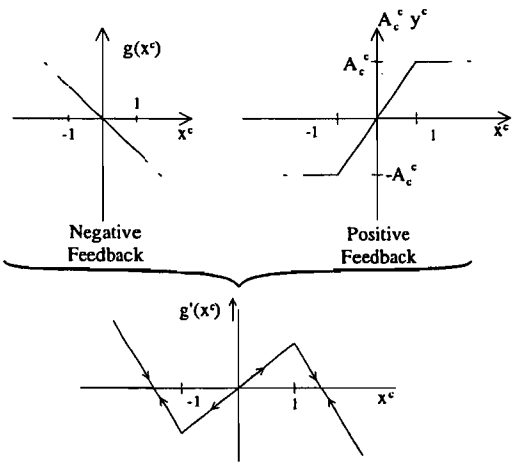

Figure 17 Chua-Yang model feedback loops combined

As can be seen from Figure 17 the value of A_c^c must be at least +1 for the system to have two distinct stable equilibrium points.

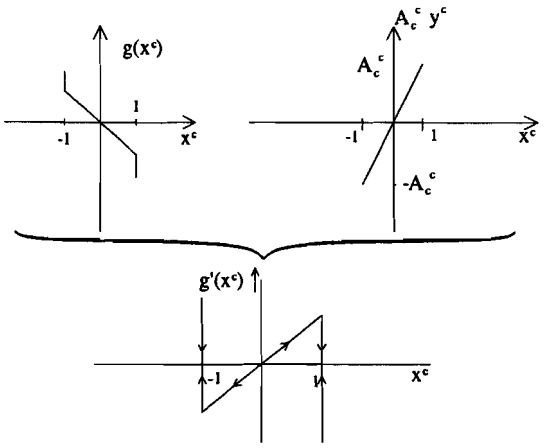

Figure 18 Full-range model feedback loops combined

For the Full Range model too there are two feedback loops which may be combined (See Figure 18). It appears that is doesn't make a difference for the stable equilibrium points how the new (combined) function $g'(x^c(t))$ is obtained (via 'Chua and Yang' or via 'Rodriguez-Vázquez'). The first assumption that is made in this Matlab program is that the new function consists of a modified function $g(x^c)$ and a self-feedback operator A_c^c (See Figure 19).

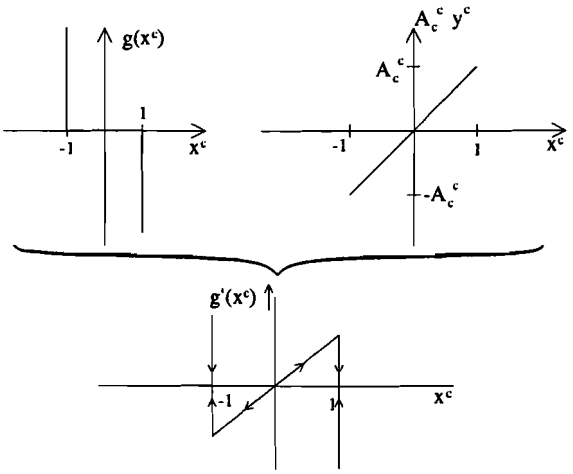

Figure 19 Alternative feedback loops with same result

This function $g(x^c)$ has an output that is $\pm\infty$ if x^c becomes ∓ 1 and is zero if $-1<x^c<1$.

The second assumption is that the time step T is chosen small enough to allow the differentiation to be replaced with the Euler forward differential operator;

$$\frac{dX}{dt} \approx \frac{X(n+1)-X(n)}{T} \tag{15}$$

Thus finding:

$$
\begin{aligned}
&C\frac{dV_x}{dt} = -\frac{V_x}{R_x} + \sum_{d\in N_r(c)} \left\{ A_d{}^c V_y{}^d(t) + B_d{}^c V_u{}^d(t) \right\} + I_c \\
&R_x C\frac{dV_x}{dt} = -V_x + R_x \sum_{d\in N_r(c)} \left\{ A_d{}^c V_y{}^d(t) + B_d{}^c V_u{}^d(t) \right\} + R_x I_c \\
&\rightarrow \frac{dV_x}{dt} = \frac{g'(V_x)}{R_x C} + \frac{1}{C} I \\
&\Rightarrow V_x(n+1) = V_x(n) + \frac{T}{R_x C} g'[V_x(n)] + \frac{T}{C} I
\end{aligned}
\tag{16}
$$

From the results it can be concluded that for CCD these assumptions are valid and that the circuit operates correctly!

For CCD something can be said with regard to the values of self-feedback operator $A_c{}^c$ since not every value is valid if a properly functioning cell is to be obtained. Assume:

$$
A = \begin{pmatrix} 0 & 0 & 0 \\ 1 & A_c{}^c & -1 \\ 0 & 0 & 0 \end{pmatrix},\ B = \begin{pmatrix} 0 & 0 & 0 \\ 0 & 0 & 0 \\ 0 & 0 & 0 \end{pmatrix} \text{ and } I = 0 \tag{17}
$$

then a cell x^c is only affected by itself and the neighbouring cells on its left- and right-hand side which will be denoted with x(l) and x(r) respectively. If these neighbouring cells are assumed to have constant output then there are four possible situations. The subsequent values for the output of cell x^c indicate whether the state value of cell x^c is stable. If $x^c(0)=+1$ and $x^c(n+1)-x^c(n)\leq 0$ then $x^c(n)$ will tend towards -1 and therefore $x^c(0)=+1$ is an instable value for the output of cell x^c. See Table 1.

Table 1 Subsequent output values of a cell

#	x(l)	x^c	x(r)	$x^c(n+1)-x^c(n)$
A	-1	+1	-1	≥0
B	-1	+1	+1	≤0
C	+1	+1	-1	≥0
D	+1	+1	+1	≥0

For situation A and D, the output of cell x^c should be stable, so (using equations (16) and (17)):

$$\begin{aligned} \frac{T}{C}A_c{}^c x^c + \frac{T}{C}g'[x^c(n)] &\geq 0 \\ A_c{}^c \cdot 1 + (1 \cdot x(l) + -1 \cdot x(r)) &\geq 0 \\ A_c{}^c &\geq x(r) - x(l) \\ A_c{}^c &\geq 0 \end{aligned} \tag{18}$$

For situation B, the output of cell x^c should become '-1' ;

$$\begin{aligned} A_c{}^c x^c + g'[X(n)] &\leq 0 \\ A_c{}^c \cdot 1 &\leq x(r) - x(l) \\ A_c{}^c &\leq 2 \end{aligned} \tag{19}$$

For situation C, the output of cell x^c should remain '+1':

$$\begin{aligned} A_c{}^c x^c &\geq g'[X(n)] \\ A_c{}^c &\geq -1 - 1 \\ A_c{}^c &\geq -2 \end{aligned} \tag{20}$$

If x^c was taken to be x^c=-1 a similar deduction could be made with the same results. Other restrictions can be found when observing the edge cells (see Table 2).

Table 2 Subsequent output values of an edge cell

#	x(l)	x^c	x(r)	$x^c(n+1)-x^c(n)$
A	0	+1	+1	≥0
B	0	+1	-1	+/-
C	0	-1	-1	≥0
D	0	-1	+1	+/-

For situation A and C, the output of cell x^c should be stable, thus finding that $A_c{}^c \geq 1$. For situation B and D, it is not clear whether x^c should keep the value it had before (denoted with '+/-' in the last column). It can be shown however that for $A_c{}^c \geq 1$, x^c will not change (and thus be 'stable'). As a result, it can be concluded that for the templates as defined earlier, the cell reaches a (stable) steady state solution if:

$$1 \leq A_c{}^c \leq 2$$

The dynamical behaviour of the cell has been verified experimentally using the Matlab program and displays a behaviour as is dictated by the properties of CCD.

4 Design at system level

There are several possibilities to represent the state of a cell. The most common representation of a state however is done by use of either a current or a voltage. There are some advantages and disadvantages to either description. If the state were to be described by a current, an inductor may be used as the differentiator. Disadvantageous is that the state of other cells must be converted to a voltage, amplified with a different gain for each cell (assuming a random template) and the results must be added. See also Figure 6. A 'pro' is that use can be made of current mirrors and that using current mirrors, an amplification factor can be implemented right away by varying the width/length ratio in the current mirrors.

If the state were to be described by a voltage, a capacitor may be used as the differentiator. In this case, the state can be distributed anywhere without having to replicate it first before distributing (using a current mirror). Another advantage is that currents can be summed easily using K.C.L.; simply leading the currents to one node suffices!

Since it appears that representing the state by a voltage leads to circuits with less components, such a circuit is searched for. As a universal CNN is to be designed, the templates must be programmable. To accomplish this, an amplifier with adjustable gain that converts voltages to currents can be realised using a differential state multiplier that consists of only three transistors. See [5] and [4]. Moreover, if the function $g(x^c)$ is observed (Figure 19) it seems that this function may be realised using 'diodes' connected to a voltage source in such a way that if the state voltage becomes less than the minimum state voltage, the corresponding diode will start to conduct. This way the current that would have discharged that state capacitor (and hence decreased the state voltage even further) is sourced into the system. Thus the state voltage is clamped to a certain lower boundary. Likewise, the other diode will start to conduct if the state voltage exceeds the voltage to which the state must be clamped.

This way not the current that (dis-) charged the state capacitor is limited (as is the case with the implementation of P. Bruin) but the state voltage itself is affected, whereas the current supplied by the multipliers and current mirrors is <u>not</u>. As a result the large

feedback loop that is present in the circuit of P. Bruin (active integrator, comparator, clipping transistors and current mirror as seen in Figure 14) can be omitted. This in return may improve stability significantly.

The circuit at system level will look like the system shown in Figure 20.

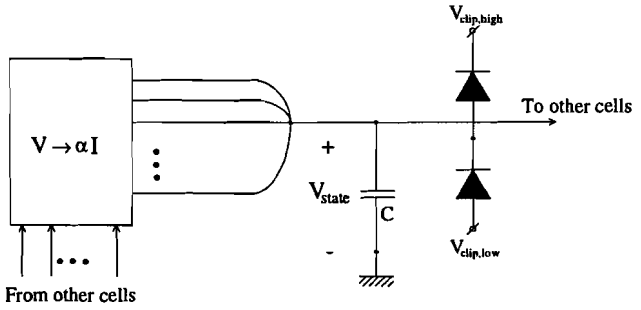

Figure 20 A cell at system level

4.1 A differential stage multiplier

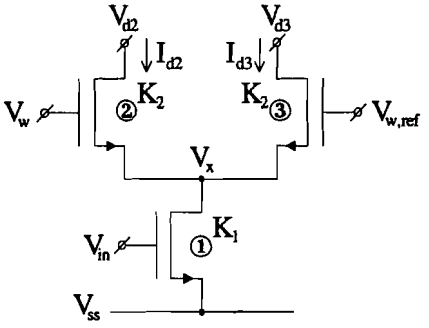

Figure 21 A differential stage multiplier

Observing Figure 21 and assuming all transistors are saturated it can be shown that, since $I_{d1}=I_{d2}+I_{d3}$:

$$K_1\left(V_{in}-V_{ss}-V_{t1}\right)^2 = K_2\left(V_w-V_x-V_{t2}\right)^2 + K_2\left(V_{w,ref}-V_x-V_{t2}\right)^2 \tag{21}$$

So:

$$V_x+V_{t2} = \frac{\left(V_w+V_{w,ref}\right)}{2} \mp \sqrt{2\frac{K_1}{K_2}\left(V_{in}-V_{ss}-V_{t1}\right)^2-\left(V_w-V_{w,ref}\right)^2} \tag{22}$$

As a result:

$$I_{d2} - I_{d3} = K_2\left[\left(V_w - V_x - V_{t2}\right)^2 - \left(V_{w,ref} - V_x - V_{t2}\right)^2\right]$$
$$= \mp\left(V_{w,ref} - V_w\right)\sqrt{2K_1K_2\left(V_{in} - V_{ss} - V_{t1}\right)^2 - K_2^2\left(V_w - V_{w,ref}\right)^2} \quad (23)$$

To determine the sign of this expression it is noted that if $V_{2+}<V_{2-}$ then $I^+-I^->0$, so:

$$I_{d2} - I_{d3} = \left(V_w - V_{w,ref}\right)\sqrt{2K_1K_2\left(V_{in} - V_{ss} - V_{t1}\right)^2 - K_2^2\left(V_w - V_{w,ref}\right)^2} \quad (24)$$

As can be seen the differential stage multiplier is not an ideal multiplier but if the second term $-K_2^2(V_w-V_{w,ref})$ is kept small with respect to the first term $2K_1K_2(V_{in}-V_{ss}-V_{t1})^2$ the multiplier operates fairly linearly. It should be noted though that channel-length modulation is neglected as are other higher order effects.

There are two possible configurations to implement a differential stage multiplier; a NMOS and a PMOS version. See Figure 22.

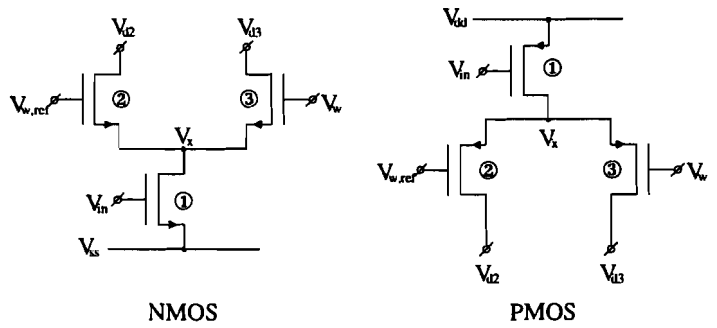

Figure 22 Two different configurations to implement a differential stage multiplier

For the NMOS configuration we can find that :

Table 3 Equations for the transistors

①	$V_{max}<V_x+V_{t1}$
	$V_{min}>V_{ss}+V_{t1}$
②	$V_{w,ref}<V_{d2}+V_{t2}$
	$V_{w,ref}>V_x+V_{t2}$
③	$V_w<V_{d3}+V_{t3}$
	$V_w>V_x+V_{t3}$

where $V_{min}\leq V_{in}\leq V_{max}$

In the cell circuit, there is a self-feedback loop and so the input of at least one multiplier will be connected with the output of the cell. If the state-voltage is connected to the gate of the tail-transistor ① and assuming V_{tn}=0.5V, we can find for transistor ①: V_{in}>0.5V, V_{in}<V_x+0.5 if V_{ss}=0V. Similarly for transistor ③: V_w<V_{in}+0.5, V_w>V_x+0.5.

So:

$$0.5<V_{in}<V_x+0.5 \tag{25}$$

and

$$V_x+0.5<V_w<V_{min}+0.5 \tag{26}$$

From (25) we obtain: $V_{max}=V_x+0.5 \rightarrow V_{max}-0.5=V_x$

Substituting into (26) we find: $V_{max}<V_w<V_{min}+0.5$. This is possible only if $V_{max}<V_{in}+0.5$ or $V_{max}-V_{min}<0.5$. If V_{min} is taken to be 0.7V then V_{max} must be less then V_{min}+0.5V=1.2V Assume $V_{in} \in [0.7;1.2]$ then:

$$V_{max} \le V_w \le V_{min} + 0.5$$
$$1.2 \le V_w \le 1.2$$

And so there's no voltage swing left for the weight-voltage. It's possible to 'transfer' some voltage swing from the state-voltage to the weight-voltage. This, however, will result in an unacceptably small voltage-swing (125mV for either voltage if the voltage swing is equally divided between state- and weight-voltage). One can try to improve this voltage swing by using different transistors (PMOS instead of NMOS). Repeating the same calculations leads to the following result:

$$V_{max} \le V_{min} + 0.5V$$

thus obtaining the same unacceptably small voltage swing. A way to increase the possible voltage swing for both the state-voltage and the weight-voltage is to use a level shifter to add/subtract a certain voltage to/from the state-voltage before applying it to the gate of the tail-transistor!

If the maximum current that will be flowing through the tail-transistor is taken to be 5μA then we can find with:

$V_{Tn}\approx 0.62V$	$\mu_n \approx 518\ cm^2/Vs$	$\varepsilon_{ox}=3.51*10^{-13}\ F/cm$
$V_{Tp}\approx -0.54V$	$\mu_p \approx 131\ cm^2/Vs$	$t_{ox}\approx 1.03*10^{-6}\ cm$

that $\frac{W_1}{L_1} \approx 0.0783$. To increase this ratio, PMOST's may be used since μ_n:μ_p=3.95:1 even though extra area has to be used for the N-well. A quick calculation shows that the ratio has increased to 0.3025. This is the reason the configuration using PMOST's is chosen, which has the additional advantage that the current mirror (that will be used to subtract the current I_{d3} from I_{d2} (see Figure 21)) will have to be made with NMOST's thereby exploiting the higher mobility of electrons!

5 Design of the cell circuit

In order to find appropriate widths and lengths for the transistors and a value for the state capacitor, the approximate input-, output- and state voltages must be known. A differential stage multiplier will be used, together with a current mirror to substract the differential current. Furthermore, the diodes that will be used to limit the state voltage to a certain maximum and minimum ('clamp' the state voltage) will be realised with transistors connected in such way that a so-called diode-configuration results. This way, the transistor will act like a diode. (See Figure 23)

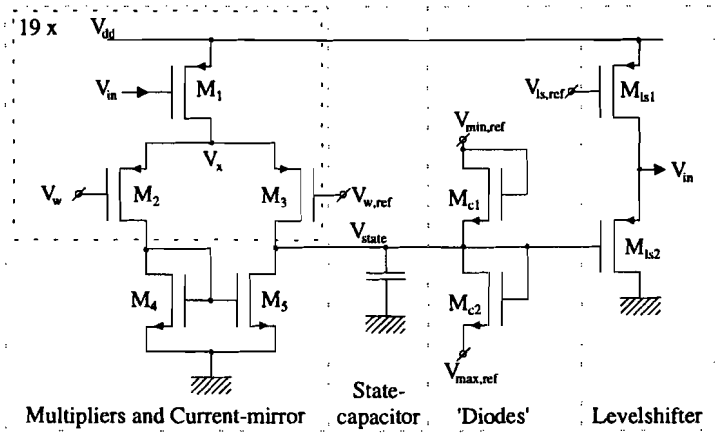

Figure 23 Schematic for a single cell of an FR-CNN

To find the voltages, voltage swing etc. two equations for every transistor will be used (one equation resulting from the fact that a transistor is saturated ($V_{gd}<V_t$) and one because it must conduct ($V_{gs}>V_t$)). If the rail voltage is taken to be V_{dd}=3.3V then one can find:

$$V_{in} \in [1.9;2.5]$$
$$V_x \leq 2.2V$$
$$V_{w,ref} \in [0.9;1.5]$$
$$V_{state} \in [0.72;1.32]$$

If the maximum current flowing through the tail transistor is set to 5μA then the W/L-ratio for the transistors can be found to be:

Transistor M_1

$$\frac{W}{L} = 0.3025$$
$$\Rightarrow \frac{W}{L} \cong \frac{1.3}{4.3}$$

Transistor M_2, M_3

$$\frac{W}{L} = 0.913$$

$$\Rightarrow \frac{W}{L} \cong \frac{1.0}{1.1}$$

Transistors M_4, M_5 (Current mirror)

$$\frac{W}{L} = 5.659$$

$$\Rightarrow \frac{W}{L} \cong \frac{6.8}{1.2}$$

The voltages $V_{ref,max}$ and $V_{ref,min}$ -which are voltages that control the potential at which the state will be clamped- are taken to be 0.70V and 1.34V respectively and can be found by assuming the state voltage is 1.32V and 0.72V respectively and assuming that the maximum possible current (95μA) flows through the diodes. The W/L-ratio for the diode transistors ('clipping-transistors') will have to be: 16.0μm/0.7μm.

Assuming a 5μA current is allowed to flow through the transistors of the level shifter, we can find that for T_{LS2}: W/L=0.5464→ W/L≈1.0μm/1.8μm and for T_{LS1}: W/L=1.7267→ W/L≈1.9μm/1.1μm.

In order to estimate the value of the capacitor that will be used as the state capacitor, it is assumed that the state capacitor must be 20 times larger than the parasitic capacitance in parallel to the state capacitor. Assuming that the parasitic capacitance of major importance is formed by the gate capacitances, the simple -approximated- function to calculate the gate capacitance can be used: $C_g = W \cdot L \cdot C_{ox}$.

To account for other parasitic capacitances, 25% to the total gate capacitance is added. Thus: $C_{g,tot} = C_{g,T_{LS2}} + C_{g,T_{C2}} = 28fF \rightarrow C_{g,tot} + 25\% = 35 \cdot 10^{-14} F$. If this value is assumed to be 5% of the total state capacitance, then C_{state} will be 0.7pF.

When simulating the circuit with the parameters given above it does not give the expected results. From this it can be concluded that the formulas that are derived from a simple model of the transistor no longer apply for the transistors that are described using Level 47 HSPICE parameters.

5.1 Obtaining modified transistor parameters

In order to maintain the possibility of calculating voltages and currents using the simple quadratic formulas, modified parameters will have to be used. To find these parameters some simulations were conducted.

The system is to be modelled with:

$$I_d = K' \cdot \frac{W}{L}\left(V_{t,p} - V_{gs}\right)^2\left(1 + \lambda\, V_{sd}\right)$$
$$\text{with } V_t = V_{t0} + \gamma\left(\sqrt{\left|V_{sb} - \varphi_s\right|} - \sqrt{\left|\varphi_s\right|}\right) \qquad (27)$$

Using [7] and LEVEL47 HSPICE parameters (p.77):

φ_s=0.8221 V, T=298.15K

n_i=1.25674*10^{10} cm^{-3}, E_g=1.11562 V

$W_{p,eff}=W_p$, $L_{p,eff}=L_p$-0.069µm

$W_{n,eff}=W_n$-0.046µm, $L_{n,eff}=L_n$-0.06µm

HSPICE simulations showed that the drain-currents of the transistors depending on the drain-, gate- and source voltages can be described fairly good with:

PMOS:

$$I_d = 1.455 \cdot 10^{-5} \cdot \frac{W_{eff}}{L_{eff}}\left(V_t - V_{gs}\right)^2\left(1 + 0.02 \cdot \frac{3.2}{L} \cdot V_{sd}\right)$$
$$\text{with: } V_t = 0.5761 + 0.663\left(\sqrt{\left|V_{sb} - 0.8221\right|} - \sqrt{0.8221}\right) \qquad (28)$$
$$W_{eff} = W,\ L_{eff} = L - 0.069\mu m$$

NMOS:

$$I_d = 7.24 \cdot 10^{-5} \cdot \frac{W_{eff}}{L_{eff}}\left(V_{gs} - V_t\right)^2\left(1 + 0.26 \cdot \frac{0.8}{L} \cdot V_{ds}\right)$$
$$\text{with: } V_t = 0.6421 + 0.56\left(\sqrt{\left|V_{sb} + 0.8221\right|} - \sqrt{0.8221}\right) \qquad (29)$$
$$W_{eff} = W - 0.046\mu m,\ L_{eff} = L - 0.06\mu m$$

5.2 Redesigning the circuits

Using the estimated transistor parameters (equations (28) and (29)) derived in paragraph 5.1 the circuit shown in Figure 23 can be redesigned. Assuming:

$$\begin{aligned} V_{in} &\in [1.9;2.3] \quad V_{LS,ref} = 2.2V \\ V_{state} &\in [0.9;1.3] \quad V_{\max,ref} = 0.26V \\ V_{w} &\in [0.6;1.3] \quad V_{\min,ref} = 2.0V \\ V_{w,ref} &= 0.95V \end{aligned} \tag{30}$$

the W/L-ratios can be found (using formulas and calculations from last paragraphs) as shown in Table 4.

Table 4 W/L-ratios of transistors

Transistor	W	L
M_1	1.1	2.1
M_2, M_3	2.1	0.8
M_4, M_5	11.9	0.8
M_{C1}	12.9	0.8
M_{C2}	8.0	0.8
M_{LS1}	1.5 (1.1)*	0.8 (1.5)*
M_{LS2}	1.1 (1.6)*	1.2 (0.8)*

However, the measures for M_{LS1} and M_{LS2} did not give the correct results. Optimising with HSPICE revealed that when using the secondary values indicated with: (.)* correct results were obtained such that if V_{state} ranges from 0.9V to 1.3V, V_{in} ranges from 1.9V to 2.3V as given in (30).

5.3 Current sourcing active diode

The role of the diodes is obvious (See Figure 23). The state voltage must be clamped to a certain level. If the state voltage lies within its range as defined in (30) then the diode should be reversed-biased and must not conduct. If for example the state voltage reaches its minimum then the diode must still not conduct, but should be no longer reversed-biased. It will be forward-biased if the state voltage decreased even further. When this happens an ideal diode would be able to source a current that is infinitely large. This however is not possible and although the increase in current will be much larger than the

decrease in state voltage, the slope of the characteristic of a diode will not be infinite. From simulations it appeared that the characteristics of the diodes (transistors in diode-configuration) are far from ideal; if a current of 95μA is sourced, the drop in state-voltage would be too large. As a result the state-voltage would not be clamped to a certain level but depends on the current that is sourced which is an undesired effect. (A current of 95μA is an extreme: every neighbouring cell, the cell itself and the constant input sourcing or draining its full current into or from the cell. Thus: 19*5μA=95μA) In order to obtain an active diode with better diode characteristics, the circuit as shown in Figure 24 can be used.

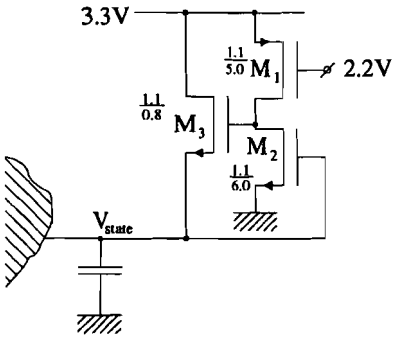

Figure 24 An active diode

If V_{state} drops and reaches its lower boundary, then transistor M_2 will be switched off, thereby no longer draining a current and its drain voltage will increase rapidly. The gate voltage of transistor M_3 is the drain voltage of M_2 and as a result M_3 will be switched on, thus sourcing a current into the state capacitor, preventing V_{state} to decrease further. The state-voltage at which M_3 is switched on, depends on the dimensions of the transistors and on the bias voltage (the gate voltage of M_1). This bias voltage also determines the gain of the amplifier consisting of M_1 and M_2 thus affecting the 'switch-on characteristic' of M_3.

The transistor that will source the actual current will be an NMOST, since the effective mobility of electrons is higher than the effective mobility of holes, resulting in smaller transistor dimensions and relatively fast switch-on characteristics.

If the circuit is simulated using the ratios as shown in Figure 24 then a DC-simulation shows that the behaviour should be satisfactory. But when a transient simulation is performed, ringing occurs. The amplitude of this ringing is unacceptably large and

should be reduced or preferably removed. To find the bias voltage on node ② (drain of transistor M_2) and have HSPICE compute the poles and zeros of the system, it has to be adjusted so that approximately 50% of the maximum current flows through transistor M_3. This is true when $V_{⑥}$=0.8972V. Using the circuit shown in Figure 25 the poles and zeros can be computed.

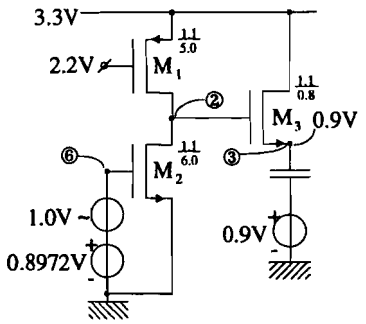

Figure 25 Schematic to obtain poles and zeros

The transfer function from ⑥ to ③ contains two poles and two zeros:

$$P_{1,2} = -7.35 \cdot 10^6 \mp j\, 823.85 \cdot 10^3 \; Hz$$
$$Z_1 = -29.78 \cdot 10^6 \; Hz, \; Z_2 = 7.10 \cdot 10^9 \; Hz$$

If the ratios of W and L of both transistors 1 and 2 are kept a constant, then the voltage at which the circuit is 'initiated' remains approximately the same. Adjusting the W/L-ratios of the transistors (but maintaining the ratio between the W/L-ratios of transistors M_1 and M_2) shows that the transfer function from ⑥ to ③ can be adjusted so that the poles are on the real axis and are positioned relatively far apart. However, ringing still occurs which is caused by the occurrence of a zero near the pole that is closest to the imaginary axis. Using HSPICE, it was seen that the location of poles and zeros depends heavily on the voltage on junction ③. Furthermore, transient analysis showed that the active diode reacted too late, that is, the switch-on time of the diode is large compare to the time needed for the circuit to fully discharge the capacitor.

The time to 'fully discharge' the capacitor (voltage drop of 0.4V) is 2.9ns which is very short indeed. To tackle this problem several solutions were considered: A) decrease the response time of the diode, B) enlarge the state capacitor, C) decrease the maximum current that has to be sourced or drained by the active diode or D) enlarge the voltage swing of V_{state}. A drawback of option B) is that this will consume a lot more area on the

chip. Performing options C) or D) will result in having to redesign the differential pair and increasing the non-linear effects of the multiplier.

If option A) is more closely looked at, it can be found that if $\left.\frac{W}{L}\right|_{transistor1} = \frac{2.6}{0.8}$, $\left.\frac{W}{L}\right|_{transistor2} = \frac{2.6}{1.0}$ and $\left.\frac{W}{L}\right|_{transistor3} = \frac{1.1}{0.8}$ the active diode works acceptably fast and the ringing has been reduced significantly. Note that an extra resistor of 0.1Ω is added in series with the state capacitor to overcome some DC-convergence problems with HSPICE. Simulations were also done using extra resistors of 1kΩ, 100Ω, 10Ω, 1Ω and even 0.001Ω. Then HSPICE reported no DC-convergence problems (although the 1kΩ and 100Ω resistors did affect the cells correct behaviour).

Now, the quiescent current through transistor M_1 and M_2 is approximately 15μA. Ringing still occurs, but when the maximum current to be drained/sourced is 95μA, there is only one 'peak'. However, simulations with HSPICE showed that there was some ringing for a maximum current of 40μA which was the worst-case situation. (See Figure 26 and Table 5)

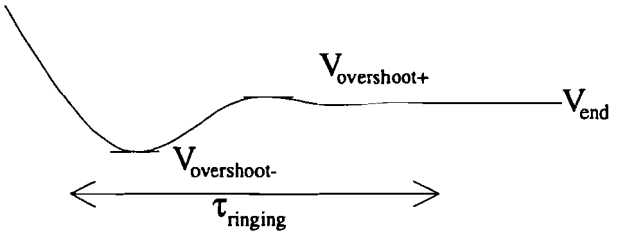

Figure 26 Ringing

Table 5 Ringing displayed for the maximum current and the worst case situation

Max. Current	$V_{overshoot-}$	$V_{overshoot+}$	V_{end}	# peaks	$\tau_{ringing}$
95μA	848.0mV	901.9mV	900.9mV	1	±6ns
40μA	882.9mV	927.2mV	914.6mV	4	±15ns

The time that is needed for the ringing to decay is small enough to accept some ringing, since the relaxation time of the system will probably be an order of magnitude larger. This may seem an invalid assumption if it is noted that the state capacitor may be fully (dis-) charged in 2.9ns. However, this can only happen if every neighbouring cell sources or drains its maximum current into (or from) the cell. Moreover, the inputs of the cells (acting via the control operator) must do so too. This situation is not very likely to happen and it was verified with HSPICE that the time needed to fully (dis-) charge the state capacitor during normal operation is an order of magnitude larger.

5.4 Current draining active diode

In order to be able to drain the maximum current and thus 'clamp' the state voltage to a certain value, an NMOS transistor will be used like in Figure 25. However, if the circuit that was used in paragraph 5.3 is transposed, difficulties arise; transistors that cannot be kept in saturation or transistors that will not conduct at all. To overcome these problems, several other circuits architectures have been tried. Now a symmetrical CMOS amplifier is used and all transistors work satisfactorily. (See Figure 27)

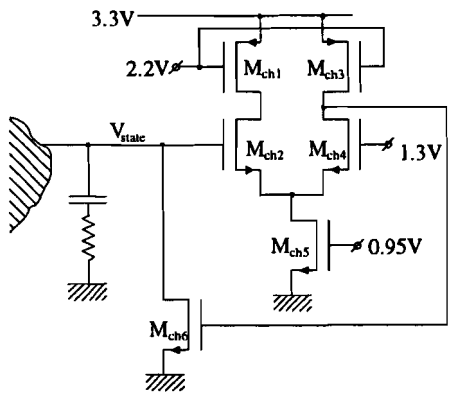

Figure 27 Schematic for symmetric current draining active diode

The use of an CMOS amplifier is disadvantageous since extra voltage sources are required. However, it has the advantage that the voltage at which the state should be clamped may be adjusted as well as the bias of the circuit. If the drain voltage of the tail-transistor M_{ch5} is chosen to be 0.4V and if its gate-voltage is set to 0.95V then V_d of M_{ch4} must be 0.6V (V_g-V_t<V_d, using (29) it is found that: V_d>0.547V) and (V_g>V_s+V_t → V_g>1.15V). In order to drain a current of 95μA through M_6, its gate-voltage must be at least 1.5V, so if this CMOS amplifier is balanced, M_{ch6} will not even conduct a

current of 95μA yet. If the quiescent current is chosen to be 12μA then the dimensions of the transistor can be found (Table 6):

Table 6 Measures of transistors used in active diode

Transistor	W (μm)	L (μm)
M_1, M_3	4.5	3.6
M_2, M_4	5.8	1.6
M_5	2.6	1.6
M_6	1.1	0.8

To find the measures that will render the circuit to function without displaying ringing, the poles and zero are computed for several W/L-ratios. It is found that the time needed to switch on transistor M_{ch6} is too short. Therefore the gain of the characteristic of the total active diode must be decreased. (That is, the switch-on characteristic must decrease.) This cannot be done by adjusting the measures of M_{ch6} as this increases the capacitive load for the CMOS amplifier (M_{ch1}...M_{ch5}) significantly, thereby disturbing its proper functioning. To decrease the gain of the amplifier M_{ch1} and M_{ch3} must be given a gate-voltage that is less than 2.2V. However, the DC-characteristic will be shifting as well and therefore the W/L-ratios will have to be adjusted as well!

It appears that the ringing, overshoot and the time needed for the ringing to decay is influenced very strongly by the measures of M_{ch6}. This will probably not be only due to the fast characteristics of the amplifier, but also due to the capacitive load that is formed by the gate of M_{ch6}. This is another reason why the dimensions M_{ch6} are kept small. To 'overcome' the effects of parasitic capacitive loads, usually the current that may (dis-) charge these loads is increased. This in return would mean an even larger CMOS amplifier gain, which is unwanted, since this would increase the switch-on time of M_{ch6}. The resulting circuit therefore will be a trade-off between high currents (resulting in some ringing) or having to deal with large parasitic capacitances which results in ringing as well.

Simulation results (Appendix A) of the circuit of Figure 27 with transistor measures as given in Table 6, show an acceptable amount of ringing (See Figure 28).

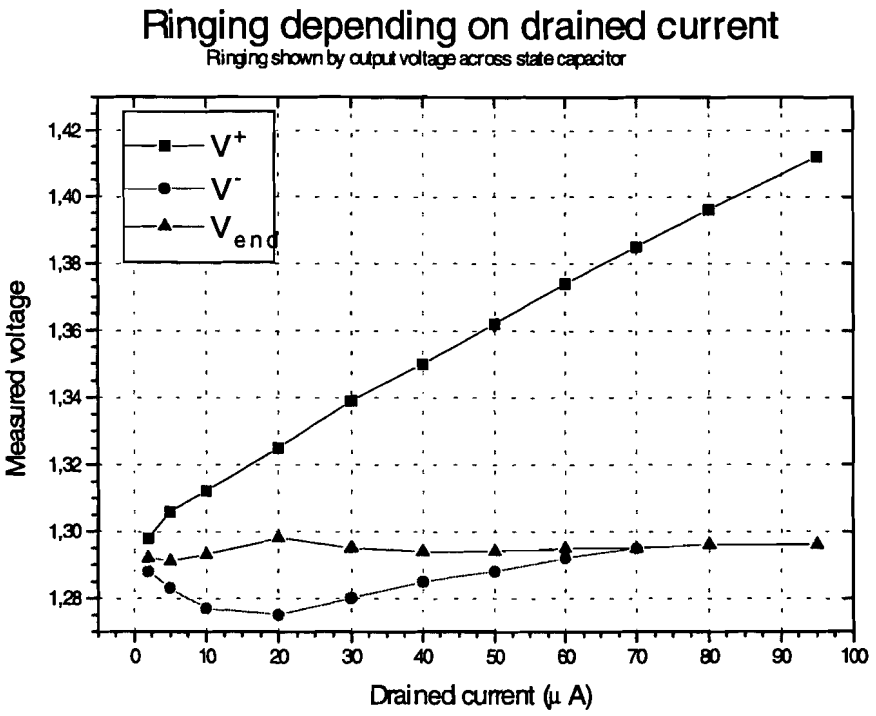

Figure 28 Amount of ringing depending on the drained current with V^+ representing $V_{overshoot+}$ and V^- representing $V_{overshoot-}$

6 The total cell circuit

A schematic of the total cell circuit is shown in Figure 29. It should be kept in mind that although only one three-transistor multiplier is shown, in the actual circuit 19 multipliers are connected in parallel, whereas only one current mirror is used!

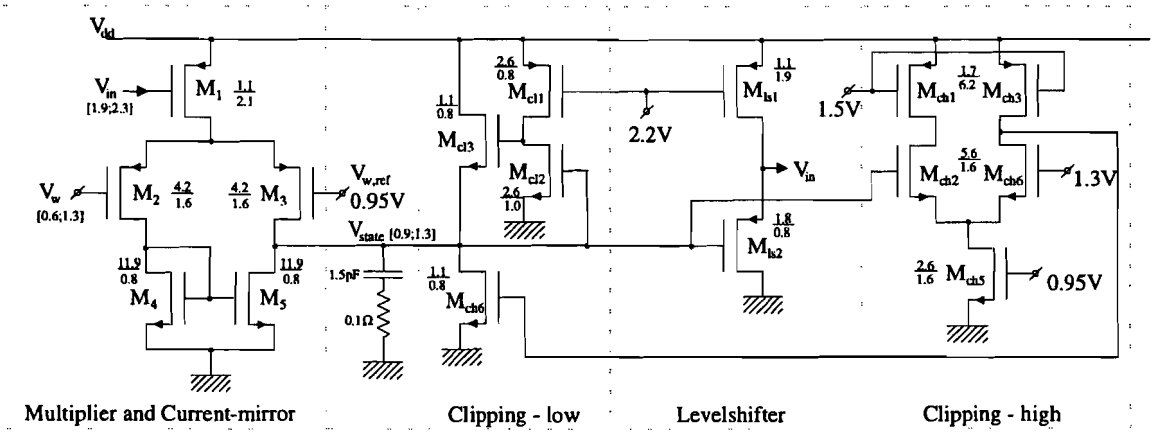

Figure 29 Schematic of the total cell circuit

Since differential stage multipliers are used, only a two-quadrant multiplier is realised. One important effect is that (with the use of the current mirror) the multiplier can only source or sink a current, with the magnitude depending on both the input voltage and weight-voltage, but the sign depends on the weight-voltage alone and cannot change 'at runtime' since the weight-voltages are constants (as the template parameters are constants!) In order to overcome this effect but still use the template parameters as given by Rodriguez-Vázquez and not the modified parameters as given in [5], an offset current is introduced. This is done in such a way that if the state voltage is exactly halfway its full range, the current sourced (or drained) by the multiplier connected to this cell is exactly counteracted by the additional constant current. This in return can be done using an other multiplier that adds the required current. The resulting current source is thus the constant current source as described in the state-equation plus or minus the required additional current. This modified current source introduces a single extra current into (or from) the cell and can be realised by a multiplier. See Figure 30.

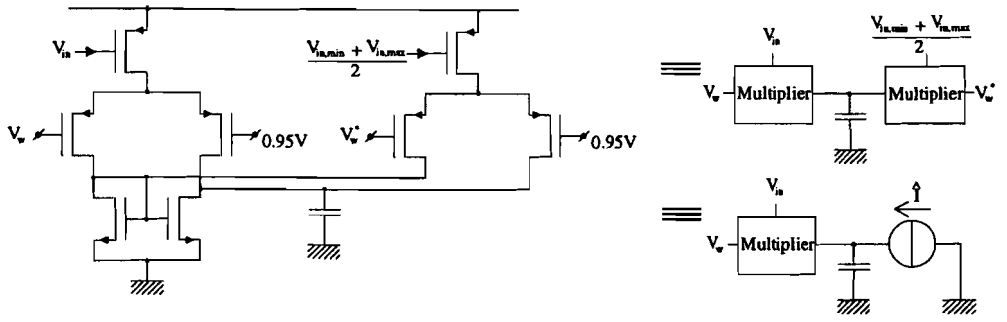

Figure 30 Using a second multiplier to account for constant current

Suppose the left-hand multiplier in Figure 30 is to realise the self-feedback parameter A_c^c. Then V_{in} will be connected to the output of the cell. The output of the cell is the shifted state voltage of the cell (due to the levelshifter). As the state voltage can range from 0.9V to 1.3V, the output of the cell should be ranging from 1.9V to 2.3V. If the state voltage is 1.1V (which would be exactly halfway its full range) the output voltage would be 2.1V. Due to non-linearities of the level-shifter, this voltage is 2.0762V as can be measured with HSPICE. So:

$$\frac{V_{in,\min} + V_{in,\max}}{2} = 2.0762V \tag{31}$$

Then V_w^* is the weight voltage that results in a current of 0μA if V_{in}=2.0762V ($\leftrightarrow V_{state}$=1.1000V)

7 Suggestions for improvement of the circuit

Unfortunately there are some drawbacks to this implementation. Despite the fact that the output impedance of a three-transistor multiplier is quite high, the output impedance of 19 multipliers in parallel is reduced significantly. Also, due to the small length of the transistors used to obtain a current mirror, the output impedance is reduced even further. See Figure 31.

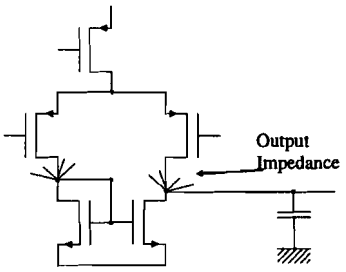

Figure 31 Reduced output impedance

This can be verified in HSPICE using the schematic shown in Figure 32 where the state capacitor is replaced with a DC-voltage source.

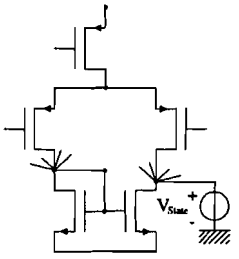

Figure 32 Schematic to obtain output impedance

The output impedance can be found to be approximately 81kΩ. However, the output impedance depends on the weight voltage that is applied as well as on the input voltage of the multipliers.

These effects can be modelled by assuming the multipliers and current mirror have an infinitely high output impedance and a resistor is placed in parallel with the state capacitor. See Figure 33.

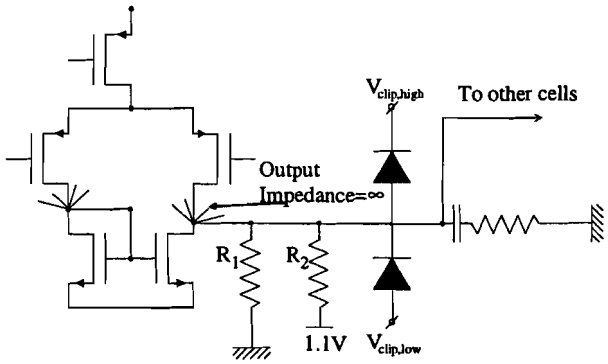

Figure 33 Model for cell-circuit with parallel resistors

It was found that the output-impedance could best be modelled with two resistors in parallel; one connected to ground ($R_1 \approx 81k\Omega$) and one connected to 1.1V ($R_2 \approx 1.2M\Omega$). Depending on the weight voltages and input voltages, the value of R_1 deviated a certain factor and can be seen as if for every multiplier with certain V_{in} and V_w a resistor (positive or negative) was placed in parallel with R_1.

If a row of six cells is simulated, it operates correctly if the self-feedback multiplier (including the offset-current-multiplier) was applied to the edge-cells three times (and for the inner cells two times!) See Appendix B for the HSPICE listing.

The effects of this fairly low output impedance can be overcome by finding the template parameters experimentally. This can be done for example by increasing the self-feedback of the cell. The extra current supplied will account for the current through the resistors, but the self-feedback parameter no longer corresponds to the parameter given by Rodriguez-Vázquez. It would be better however not to have such a low output impedance at all. The circuits that may be used to achieve a higher output impedance are shown in Figure 34.

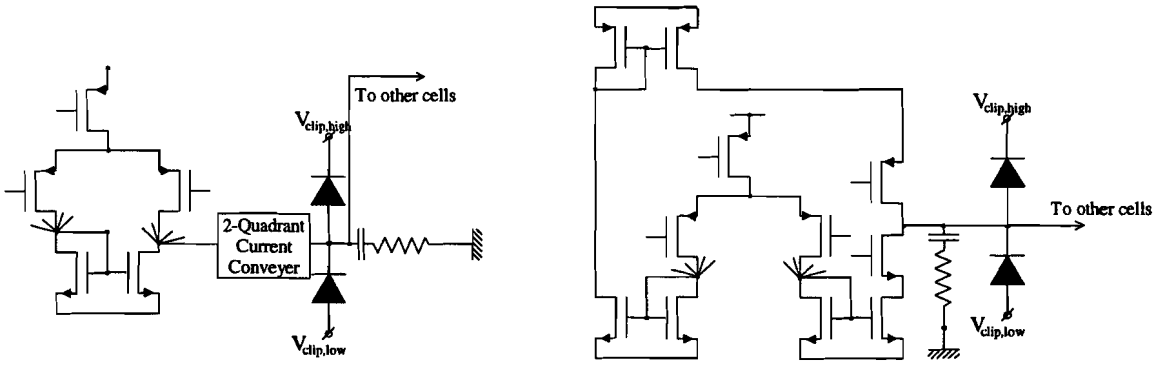

Figure 34 Schematics of circuits to improve output impedance

7.1 Results of improvements

For the implementation of the schematic using a 2-quadrant current conveyor, the circuit as shown in Figure 35 was suggested. The upper four transistors are to be observed for negative values of I_{in}.

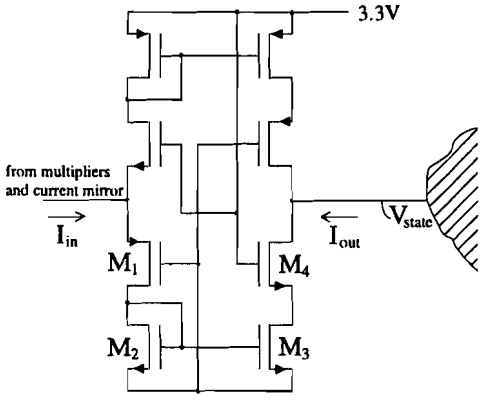

Figure 35 A 2-quadrant current conveyor

If $I_{in}>0$ then the lower four transistors must be observed. Cascode transistor M_4 is inserted in order to obtain a high output impedance. The output of the current conveyor is connected to the state capacitor and a high output impedance will prevent unintended (dis-)charging of the state capacitor. If M_4 must be saturated, then:

$$V_g < V_d + V_t$$

The source-voltage of $M_4 \neq 0$ as can be seen from Figure 35 and so $V_{t,M4} \geq 0.64V$. $V_g = V_{dd}$ and as a result:

$$V_{dd} < V_{state} + V_t$$
$$3.3V < 0.9V + 0.64$$

This is not true and so M_4 is not saturated. As a result the output of the current conveyor has not a high impedance. Therefore this circuit will not be used. However, if M_1, M_4 and the transistors directly above them were connected to additional voltage sources, this circuit may be used as a 2-quadrant current conveyor. This however is left for future studies.

For the implementation using current mirrors the second schematic in Figure 34 may be used. See Figure 36.

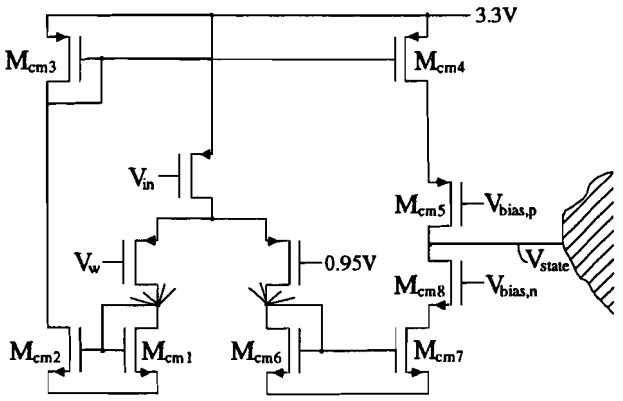

Figure 36 Schematic of cell circuit with current mirrors

As can be seen, the currents from the multiplier are mirrored using three currents mirrors. At the output of the system the currents mirrors are connected in such way that a so called push-pull configuration is obtained (M_{cm4} and M_{cm7}). Extra transistors are inserted to assure a high output impedance. The state capacitor is connected to the drains of M_{cm5} and M_{cm8}.

From the output of the multipliers a low impedance is seen, since these are connected to the drains of M_{cm1} and M_{cm6} which are always saturated.

In order to find the bias voltage $V_{bias,n}$, assume that the current through M_{cm6}=95μA. It is found that the drain voltage of M_{cm3} is approximately 0.91V. The drain voltage of M_{cm7} will be approximately 0.91V as well. Since M_{cm8} must conduct, it can be found that if its source voltage has a maximum of 0.91V, $V_{bias,n} \geq 1.8287V$. Likewise it can be found that $V_{bias,p} \leq 1.1823V$ if the current through M_{cm4} is taken to be 95μA.

When the circuit was simulated it was found that the current mirrors consisting of M_{cm3}, M_{cm4} and M_{cm6}, M_{cm7} functioned properly if $V_{bias,p}$=1.16V and $V_{bias,n}$=1.84V.

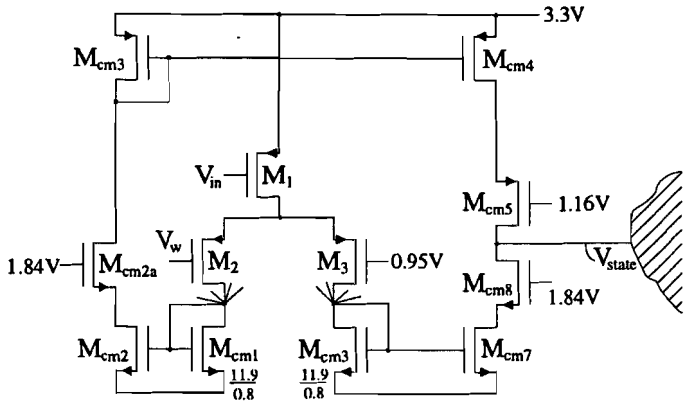

Figure 37 Schematic of cell circuit with more accurate current mirrors

It was seen however that the current through M_{cm2} mismatched the current through M_{cm1} with about 2μA. To overcome this problem, an extra transistor was inserted. See Figure 37. Now all the current mirrors functioned well and a DC-simulation showed that the currents were mirrored with a deviation of maximally ±0.02μA. The maximum current of 95μA must be mirrored and in order to do so the transistors used to mirror a current must have equal dimensions. This however causes the chip area needed for the total cell circuit to increase significantly. This expansion can be reduced if the width of the transistors M_{cm2}, M_{cm2a}, M_{cm3}, M_{cm4}, M_{cm5}, M_{cm7}, M_{cm8} is halved. (→ W/L=6.0μm/0.9μm) As a result, the maximum current that (dis-) charges the state capacitor has decreased by a factor two as well. This has its effects on the speed with which the cell operates (it becomes 'slower'), but has its positive effects on the output impedance (which increases).

It was found that if V_w=0.9503V the multipliers are balanced and there is no current flowing through the state-capacitor. If the state voltage is varied (using a DC-voltage source which replaces the state capacitor) it is found that the resulting current through the DC-voltage source is 18.0nA@V_{state}=0.950V and -2.0nA@V_{state}=1.250V. (See Appendix C). From this it is easily calculated that the output impedance is ≈15MΩ.

It was seen that the maximum current that can be drained and sourced using only one multiplier is 2.7812μA. The largest template parameter P_{max} must thus represent a current of 2.7812μA. If P_{max}=1.5 as is the case with the CCD-example, then A_c^c should

correspond with a template parameter of 1.5. The weight voltage of the multiplier realising the self-feedback must be 1.3V. This is shown quite easily; if V_{state} rises then V_{in} rises as well. As a result the tail transistor M_1 sources a smaller current. The current source that is needed to counteract the current offset -due to the use of a two-quadrant multiplier (and the template parameters given by Rodriguez-Vázquez)- must then source a current into the state capacitor (thereby increasing the state voltage). The self-feedback multiplier must drain a smaller current and thus it can be concluded that positive values for template parameters correspond to higher weight-voltages.

It is found that V_W=1.3V corresponds to P=P_{max}=1.5 and 0.6170V corresponds to P=--1.5. If the maximum current of 2.7812μA corresponds to P=1.5 then P=1.0 corresponds to 1.8541μA. It was found experimentally that for P=1 the weight voltage must be 1.1450V and for P=-1, V_w=0.7620V.

If a cell is only connected to itself (only A_c^c is present) it is found that if the initial state voltage=1.11V, the resulting output of the cell is high, while if the initial state voltage is 1.09V, the resulting output of the cell is low.

A row of six cells connected in such way that it performs connected component detection was simulated and operates properly. See Table 7 for some experiments that were conducted.

Table 7 Experiments conducted with a row of 6 cells. Function: Connected component detection without additional edge-cells

$V_{state}(t=0)$ Initial conditions of subsequent cells in row of 6 cells ('0'=0.9V, '1'=1.3V)	$V_{state,steady\ state}$ Results of subsequent cells in row of 6 cells ('0'=0.921V, '1'=1.29V)	Settling time Steady state reached after:
011110	000010	1.3µs
101100	111010	1.5µs
001111	000001	1.3µs
001000	000010	1.6µs
101000	111010	2.0µs
111000	111110	1.0µs
111111	111111	<400ns
000000	000000	<50ns
001100	000010	1.0µs
100000	111110	2.0µs

Note that the voltage at which the state is clamped is somewhat higher than 0.9V. This is caused by the current sourcing active diode. (For the effects of this diode, see also Appendix C). The characteristics of this diode may be improved by using an active diode like the present current draining active diode and is left for future studies. Nevertheless the results are promising and although the output impedance is quite high, the speed at which the network operates can be increased by increasing the maximum current that can be supplied to 95µA while keeping a high output impedance.

8 Theory: boundary of the basin of attraction

The state voltage of a cell in a CNN varies as a function of time, due to self-feedback and interaction with other cells. Because of these interactions, the state voltage will not necessarily decrease or increase monotonically. The state voltage can be plotted as a function of time as is done in Figure 16; for every individual cell the state voltage (on the Y-axis) is plotted against time (X-axis). If a CNN consisting of only two interacting cells is considered, it is possible to plot in a convenient way one state voltage versus the other thus obtaining a state space plot. Although the state voltages are dependent of the time, they are now not explicitly plotted as a function of time. In Figure 38, V_{S1} and V_{S2} are the state voltage of the two cells. This state-space plot enhances the insight in the dynamical behaviour of the system rather than the state voltage plotted versus time (a 'time-diagram').

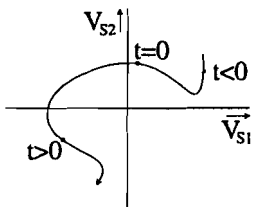

Figure 38 Plot of a trajectory in state space

As time changes, so too will the state voltages. If subsequent points in state space are connected a curve is obtained and is called the 'trajectory' of the system. If this was done for three interacting cells in a CNN, then for a complete description of the dynamical behaviour, a three dimensional space would have to be drawn since there are three state-voltages to be plotted.

Considering a CNN consisting of two cell, it is possible to find a certain 'border' separating the entire state space (two dimensional in our example) into two regions, so that if the system starts in any point of one region, it will always converge to one specific equilibrium point, while if it starts in any other point, the system will always converge to the other equilibrium point. This 'border' is called the 'boundary of attraction' for obvious reasons and the region it encapsulates is called the basin of attraction.

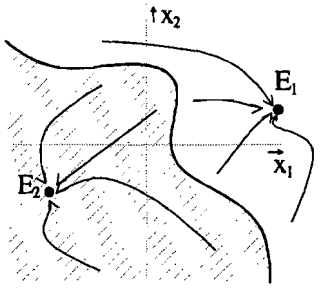

Figure 39 Separation of the state space

In Figure 39 a two-dimension state space is depicted containing two equilibrium points (E_1 and E_2). The basin of attraction for E_2 is shaded and the white area is the basin of attraction for E_1. The border between them (drawn with a thick line) is the boundary of attraction. The objective is to find a description for this border and thus be of help in explaining the outcome of the neural network.

9 The Lyapunov energy function

If a CNN is considered that consists of two cells, then a two dimensional state space displays the dynamic behaviour of the cells. Assume that a cell is described by the regular state equation. (See also (2))

$$C\frac{dV_x(t)}{dt} = -\frac{V_x(t)}{R_x} + A_c{}^c V_y(t) + \sum_{\substack{d\in N_r \\ d\neq c}} A_d{}^c V_y{}^d(t) + \sum_{d\in N_r} B_d{}^c V_u{}^d + I \tag{32}$$

Or:

$$R_x C\frac{dV_x(t)}{dt} = -V_x(t) + R_x A_c{}^c V_y(t) + R_x \sum_{\substack{d\in N_r \\ d\neq c}} A_d{}^c V_y{}^d(t) + R_x \sum_{d\in N_r} B_d{}^c V_u{}^d + R_x I \tag{33}$$

To obtain a dimensionless equation, the voltages can be normalised with:

$$\frac{V_x}{V_{\max}} = x^c,\ \frac{V_y}{V_{\max}} = y^c,\ \frac{V_u}{V_{\max}} = u^c$$

So dividing (33) by V_{max} gives:

$$R_x C\frac{dx^c(t)}{dt} = -x^c(t) + R_x A_c{}^c y^c(t) + R_x \sum_{\substack{d\in N_r \\ d\neq c}} A_d{}^c y^d(t) + R_x \sum_{d\in N_r} B_d{}^c u^d + \frac{R_x I}{V_{\max}} \tag{34}$$

If the time is normalised as : $t=R_xC\tau$ then

$$\frac{dx^c(\tau)}{d\tau} = -x^c(\tau) + R_x A_c{}^c y^c(\tau) + R_x \sum_{\substack{d\in N_r \\ d\neq c}} A_d{}^c y^d(\tau) + R_x \sum_{d\in N_r} B_d{}^c u^d + \frac{R_x I}{V_{\max}} \tag{35}$$

which can be rewritten to obtain:

$$\frac{dx^c(t)}{dt} = -x^c(t) + a_c{}^c y^c(t) + \sum_{\substack{d\in N_r \\ d\neq c}} a_d{}^c y^d(t) + \sum_{d\in N_r} b_d{}^c u^d + i^c$$

$$\text{with: } a_c{}^c = R_x A_c{}^c,\ a_d{}^c = R_x A_d{}^c,\ b_d{}^c = R_x B_d{}^c,\ i^c = \frac{IR_x}{V_{\max}} \tag{36}$$

This normalised state equation (36) facilitates the description of the individual cell equations. Assume that the two-cell CNN is described by:

$$\begin{aligned} \dot{x}_1 &= -x_1 + 1.5y_1 + y_2 + 1 \\ \dot{x}_2 &= -x_2 + y_1 + 1.5y_2 + 1 \end{aligned} \tag{37}$$

Here, $y_k=f(x_k)$ is the output of cell k ($k \in \{1,2\}$), which is the saturation function described in chapter 2. The 2-dimensional state space is divided into nine separate regions due to the fact that the output of a cell is a 3-segment piecewise linear function. This can be seen in Figure 40. The states are plotted along the (dashed) axes. If the horizontal axis is observed (along which x_1 is plotted) it can be seen that the state space is divided into three regions (thick vertical lines) because the output saturates. Likewise state x_2 divides the state space three regions too, thus the entire state space is divided into nine regions. If a state variable is said to be saturated, then actually the output is saturated. (For FR-CNN's this is the same.) When the output of a cell saturates the term of the output used in the state equations becomes a constant and therefore plays no longer an active role in the equations. If the magnitude of both state-variables exceeds unity, the output of both cells are saturated and the corresponding regions {1,3,7,9} are called 'saturated regions'. If only one output is saturated the corresponding regions {2,4,6,8} are called 'partially saturated regions'. If none of the outputs are saturated the system is operating in region {5}, which is called 'linear region'.

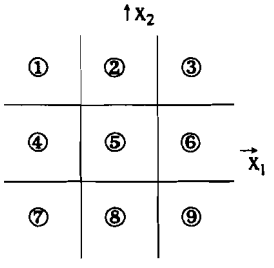

Figure 40 State space divided into nine regions

As is shown by Chua and Yang [2] and [8] the CNN (subjected to some restrictions) has stable equilibrium points which must lie in one of the saturated regions. These equilibrium points can be found by considering the saturated regions and stating that the state-variable does no longer vary. ($\dot{x}_k = 0$, $k \in \{1,2\}$) Thus, using the given state equations (37) two equilibrium points can be found ; E_1=(3.5, 3.5) and E_2=(-1.5, -1.5).

In order to find the boundary of the basin of attraction ('BOA') separating the basins of attraction of both equilibrium points, the Lyapunov energy function as defined by Chua and Yang [2] (see also [9],[10] and [11]) can be used and is described by the scalar function (38)

$$\begin{aligned} E(t) = &-\frac{1}{2}\sum_{(i,j)}\sum_{(k,l)} A(i,j;k,l)v_{yij}(t)v_{ykl}(t) + \frac{1}{2R_x}\sum_{(i,j)}\left(v_{yij}(t)\right)^2 \\ &-\sum_{(i,j)}\sum_{(k,l)} B(i,j;k,l)v_{yij}(t)v_{ukl} - \sum_{(i,j)} I v_{yij}(t) \end{aligned} \tag{38}$$

Or (using (36)):

$$\begin{aligned} \tilde{E}(t) &= \frac{E(x(t))}{V_{\max}^{\ 2}} R_x \\ &= -\frac{1}{2}\sum_{(i,j)}\sum_{(k,l)} a_d{}^c y_{ij}(t) y_{kl}(t) + \frac{1}{2}\sum_{(i,j)}\left(y_{ij}(t)\right)^2 \\ &\quad -\sum_{(i,j)}\sum_{(k,l)} b_d{}^c y_{ij}(t) u_{kl} - \sum_{(i,j)} i^c y_{ij}(t) \end{aligned} \tag{39}$$

This energy function is only valid when CNN's with symmetrical templates are used, that is, if A(i,j;k,l)=A(k,l;i,j). Chua and Yang also showed that this scalar function E(t) is a monotone decreasing function of time. For the two-cell CNN in our example, the energy function in the linear region becomes:

$$\tilde{E}(x_1, x_2) = -\frac{1}{4}\left((x_1)^2 + (x_2)^2\right) - x_1 x_2 - x_1 - x_2 \tag{40}$$

Observe that in region {5}

$$\text{grad}\,\tilde{E}(x_1, x_2) = \begin{pmatrix} -\frac{x_1}{2} - x_2 - 1 \\ -\frac{x_2}{2} - x_1 - 1 \end{pmatrix} \tag{41}$$

whereas the state equations are given by:

$$\begin{cases} \dot{x}_1 = \frac{x_1}{2} + x_2 + 1 \\ \dot{x}_2 = \frac{x_2}{2} + x_1 + 1 \end{cases} \tag{42}$$

The energy function for this two-cell CNN can be plotted as if it were a function of x_1 and x_2. Therefore the gradient of $\tilde{E}(x_1,x_2)$ shows where the slope of the energy has a maximum (that is, increases fastest). In the opposite direction, the energy function shows the largest decrease. If this energy function can be written as a scalar function (depending on x_1 and x_2) then $-\text{grad}\,\tilde{E}(x_1,x_2)$ indicates the direction of the largest decrease in energy and the direction of the actual trajectory, since these directions are the same (see (41) and (42)). This is true for our particular example and may not be true in general because energy functions might be found where the direction of the actual trajectory does not correspond to the largest decrease in energy. It is assumed however that the direction of the trajectory corresponds to the largest decrease in energy throughout this entire report unless stated otherwise. This is an important assumption and narrows down the diversity in CNN's that may be observed, because it is not necessary for a CNN to 'follow' that path in state space where the decrease in energy is largest. Metaphorically speaking, it can be seen as if the state space contains a mountain-ridge (with the altitude depending on the amount of energy). Since the energy of the CNN (altitude on the mountain) as a function of time is a monotone decreasing function, the mountain can never be ascended but is always descended. As a result, following the trajectory we can never gain 'kinetic energy' because if that were possible, it would be possible to ascend the mountain (thereby losing again the gained kinetic energy).

However, when the energy function is plotted in the saturation regions it is easily shown that the energy function remains at the same level throughout the entire saturated region. (See Figure 41) This is logical since the energy only depends on the output of the cell states which are constants in the saturated regions. This in return would mean that once the system has entered a saturated region it will not proceed to approach an equilibrium point or pass through this region at all. This is not true since the system will approach an equilibrium point or pass through a saturation region. So here, the used Lyapunov energy function does not represent a correct energy function in the sense that it 'explains' the systems behaviour.

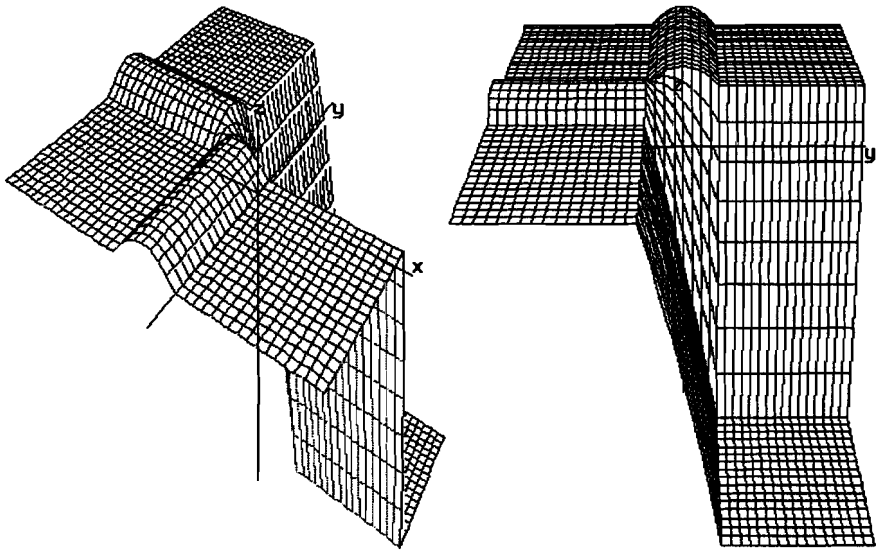

Figure 41 Lyapunov Energy function for our example (using (37) and (39)) observed from different angles, with x and y being the states (x_1 and x_2) and z representing the amount of energy.

9.1 The BOA in the linear region

If the linear region is observed the Lyapunov energy function (40) may be used since it describes a correct energy function for our example. As can be seen from Figure 41, there's a maximum within the linear region. To find this maximum in energy it is clear that, although due to noise practically unrealisable, a system that starts exactly at this maximum will not start to 'move'. This is an other equilibrium point but -unlike the ones in the saturated regions- it is unstable. This equilibrium point can be found however by stating that $\dot{x}_1 = 0$ and $\dot{x}_2 = 0$. Thus the maximum in energy is obtained for $x_1 = -\frac{2}{3}$ and $x_2 = -\frac{2}{3}$. From this point, the system can follow trajectories that lead in every direction. This is true, since the trajectories follow the (opposite direction of the) gradient defined by the energy function (as no 'mass' is involved and so no kinetic energy is gained). It may not be true with other two-cell CNN's where other template parameters are used. (The constant factor with which the output of a cell affects the state of an other cell is called a template parameter.) To overcome this problem, a 'force' is introduced. If this system is submitted to a force-field depending on the exact position in the state-space, the energy-function is no longer needed to describe the systems behaviour. Again speaking in metaphors; if a ball is placed on a mountain it will start to roll towards a certain direction directed by a force that depends on 1) the gravitational force (which is assumed to be a constant) and 2) the orientation of the mountain. In

Figure 42 the mountain representing the energy as a function of the states x_1 and x_2 is plotted, as well as a 'ball' on its surface. The force acting on the ball is projected on the x_1,x_2-surface (the trajectory) and decomposed into its components along x_1 and x_2 respectively.

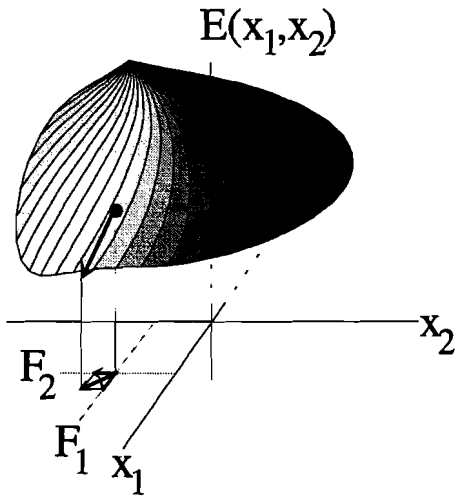

Figure 42 Force composed of two directional components

If the force field is taken in such a way that it always describes the correct direction to which the trajectory tends, the state equations can be used. Therefore, introduce:

$$\underline{F} = F_1 \cdot \underline{i} + F_2 \cdot \underline{j} = \dot{x}_1 + \dot{x}_2 \tag{43}$$

Here, F_1 does not necessarily correspond directly to $\dot{x}_1$ since F_1 can be composed of two components of force. This is logical since $\dot{x}_1$ not only depends on x_1 but also on x_2 and vice versa. (See Figure 43)

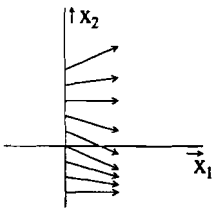

Figure 43 Dependence on both state values

Since the system is described by the state-equation as is the 'force' the two descriptions may both be used to do so. It will therefore describe the systems behaviour well, also in saturated regions (which is trivial as the state equations are used) whereas the energy function is no longer useful. This can be proven quite simply.

If there is a function f, such that:

$$\underline{F} = \text{grad}\, f \text{ with } \underline{F} = F_1 \cdot \underline{i} + F_2 \cdot \underline{j} \tag{44}$$

and if $F_1(x,y)$ and $F_2(x,y)$ have continuous first-order partial derivatives then if:

$$\begin{aligned} &\int_C \left(F_1 dx + F_2 dy\right) = 0 \text{ (independent of the path "C")} \\ &\leftrightarrow \underbrace{\text{curl}\,\underline{F} = 0}_{\frac{\partial F_2}{\partial x} = \frac{\partial F_1}{\partial y}} \end{aligned} \tag{45}$$

the system ($\underline{F}$) is called conservative (since $\text{curl}\,\underline{F} = \text{curl}(\text{grad}\, f) = 0$). [12]

If $\underline{F}$ is not conservative, then the energy at a certain point depends on the trajectory that was followed. It is then impossible to define a fixed amount of energy for this point and thus the energy function cannot be represented by simply a scalar function. As an example, assume that x_2 is saturated ($x_2 \leq -1$), then:

$$\begin{cases} \dot{x}_1 = -x_1 + a_1^{\,1} x_1 - a_2^{\,1} + B_1 \\ \dot{x}_2 = -x_2 + a_1^{\,2} x_1 - a_2^{\,2} + B_2 \end{cases} \tag{46}$$

So:

$$\left.\begin{aligned} F_1 &= \left(a_1^{\,1} - 1\right) x_1 - a_2^{\,1} + B_1 \\ F_2 &= -x_2 + a_1^{\,2} x_1 - a_2^{\,2} + B_2 \end{aligned}\right\} \begin{aligned} \frac{\partial F_1}{\partial x_2} &= 0 \\ \frac{\partial F_2}{\partial x_1} &= a_1^{\,2} \neq 0 \end{aligned} \tag{47}$$

And so $\underline{F}$ is not conservative conform (44). In region {8} the energy function cannot be described by a simple scalar function. The energy in a certain point in state space would be depending on the path (the trajectory) that was followed. This cannot be true for a CNN and leads to the conclusion that the assumption that the systems always follows the steepest path on the energy function towards the equilibrium points is incorrect. This implies that a scalar function may be found to represent the energy function, but then the gradient will <u>not</u> be equal to the state-equations as was the case with (41) and (42).

So far, the 'top' in energy in the linear region has been found for our particular example under the assumption that the trajectory always corresponds to the steepest descent along the energy-mountain and a 'force' has been defined (corresponding to the state equations). How does this lead to the BOA? To answer this question the characteristic is used the ridge of a mountain passes the top of the mountain and is the route with the smallest slope. Any deviation from that route will result in less energy and thus lead away from the ridge. (See Figure 44). Following this route it is like continuously balancing on this mountain-ridge.

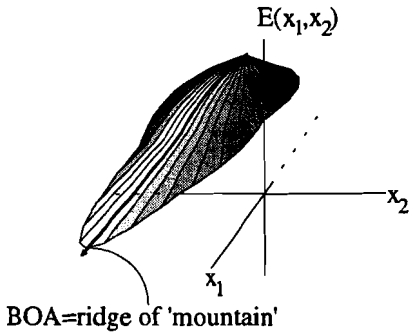

Figure 44 A special trajectory; the ridge of the mountain

To find this route (which is a special trajectory) at the edges of the region, a sort of 'work-function' may be introduced, analogues to the work done by a force.

$$W = \int_C F \cdot dr \tag{48}$$

Following the edges of the linear region the work done in order to do so can be studied. If there's a maximum on the edge it can be found by integrating the force along the edge to this point. Integrating to any other point will result in a work function that is less if there's only one maximum. If multiple extremes are found the global maximum must be observed. When the edge of the linear region with x_1=-1 is observed then, for our example:

$$W = \int_{-1}^{a} F \cdot dr = \int_{-1}^{a} (\dot{x}_1 + \dot{x}_2) dx_2$$

$$= \int_{-1}^{a} \left[\underbrace{(A_1 + a_1^{\,1} + a_1^{\,2})}_{\alpha} x_1 + \underbrace{(a_2^{\,1} + A_2 + a_2^{\,2})}_{\beta} x_2 + \underbrace{B_1 + B_2}_{\gamma} \right] dx_2$$

with
$$\dot{x}_1 = A_1 x_1 + a_1^{\,1} x_1 + a_2^{\,1} x_2 + B_1$$
$$\dot{x}_2 = A_2 x_2 + a_1^{\,2} x_1 + a_2^{\,2} x_2 + B_2$$

and A_1=-1, A_2=-1 since the linear region is observed! The integration of the force along the edge is depicted in Figure 45.

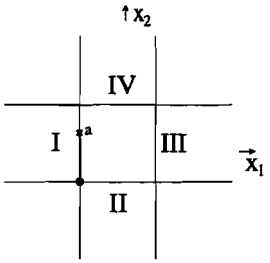

Figure 45 Integration along edge I of linear region

Thus finding:

$$\begin{aligned} W &= \int_{-1}^{a} \left[\alpha x_1 + \beta x_2 + \gamma\right] \mathrm{d}x_2 \\ &= \frac{\beta}{2} a^2 + \left(\gamma + \alpha x_1\right) a - \frac{\beta}{2} + \left(\gamma + \alpha x_1\right) \end{aligned} \tag{49}$$

To find the point where the maximum work is done, differentiate the work function to 'a' and state that the result is zero (simply finding an extreme). This has the advantage that any constants that are introduced by the force are annihilated. It is therefore not necessary to know the absolute value in energy at a certain point since only differences are observed.

$$\frac{dW}{da} = 0 \rightarrow a = -\frac{\gamma + \alpha x_1}{\beta} \tag{50}$$

and because x_1=-1, $\alpha = \frac{3}{2}, \beta = \frac{3}{2}, \gamma = 2$ it can be found that $a = -\frac{1}{3}$ so there is a BOA through (-1, $-\frac{1}{3}$).

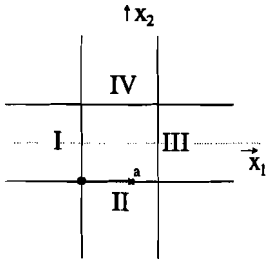

Figure 46 Integration along edge II of linear region

For edge II, the same calculation can be performed (see also Figure 46):

$$W = \int_{-1}^{a} (\dot{x}_1 + \dot{x}_2) dx_1 \; ; \quad \frac{dW}{da} = 0$$

and with x_2=-1, $\alpha = \frac{3}{2}, \beta = \frac{3}{2}, \gamma = 2$ it can be found that $a = -\frac{1}{3}$ so there is a BOA through $(-\frac{1}{3}, -1)$.

For edge III it is found that $a = -\frac{7}{3}$ which is not a valid value since it does not lie in the linear region. Likewise, for edge IV, $a = -\frac{7}{3}$ which is an invalid value too.

9.2 Obtaining the description of trajectories

To determine the trajectory through (-1, $-\frac{1}{3}$) and $(-\frac{1}{3}, -1)$ it is possible to solve the state equations for the linear region.

$$\left.\begin{aligned} \dot{x}_1 &= \frac{x_1}{2} + x_2 + 1 \\ \dot{x}_2 &= \frac{x_2}{2} + x_1 + 1 \end{aligned}\right\} \Rightarrow \begin{aligned} \underline{\dot{x}} &= A\underline{x} + \underline{h} \\ &= \begin{pmatrix} \frac{1}{2} & 1 \\ 1 & \frac{1}{2} \end{pmatrix} \underline{x} + \begin{pmatrix} 1 \\ 1 \end{pmatrix} \end{aligned} \tag{51}$$

If A has 'n' distinct eigenvalues, then A has a basis of 'n' eigenvectors. Solving det(A-λI)=0 gives: $\lambda_1 = \frac{3}{2}$ and $\lambda_2 = -\frac{1}{2}$. Substituting λ=λ_1 and λ=λ_2 into det(A-λI)=0 results in two eigenvectors: $\underline{Y}_1 = \begin{pmatrix} 1 \\ 1 \end{pmatrix}$ and $\underline{Y}_2 = \begin{pmatrix} -1 \\ 1 \end{pmatrix}$ hence:

$$Y = \begin{pmatrix} 1 & -1 \\ 1 & 1 \end{pmatrix} \qquad \begin{matrix} \uparrow & \uparrow \\ Y_1 & Y_2 \end{matrix} \tag{52}$$

Diagonalisation of A gives [12]:

$$D = Y^{-1}AY = \begin{pmatrix} \lambda_1 & 0 \\ 0 & \lambda_2 \end{pmatrix} \tag{53}$$

If $\underline{x} = Y\underline{z}$ then:

$$\begin{aligned} Y\dot{\underline{z}} &= AY\underline{z} + \underline{h} \\ \dot{\underline{z}} &= Y^{-1}AY\underline{z} + Y^{-1}\underline{h} \\ &= D\underline{z} + Y^{-1}\underline{h} \end{aligned} \tag{54}$$

From this it can be found that:

$$\begin{cases} \dot{z}_1 - \frac{3}{2}z_1 = 1 \\ \dot{z}_2 + \frac{1}{2}z_2 = 0 \end{cases} \Rightarrow \begin{cases} z_1 = -\frac{2}{3} + Ke^{\frac{3}{2}t} \\ z_2 = C_2 e^{-\frac{1}{2}t} \end{cases} \tag{55}$$

And thus (using $\underline{x} = Y\underline{z}$):

$$\begin{aligned} x_1 &= -\tfrac{2}{3} + Ke^{\frac{3}{2}t} - C_2 e^{-\frac{1}{2}t} \\ x_2 &= -\tfrac{2}{3} + Ke^{\frac{3}{2}t} + C_2 e^{-\frac{1}{2}t} \end{aligned} \tag{56}$$

These equations describe the trajectories as a function of time for the linear region. To find the trajectory through $(-1, -\frac{1}{3})$, this point can simply be substituted which then determines the constants, assuming the trajectory is in $(-1, -\frac{1}{3})$ at time t=0. Thus we can find: K=0 and $C_2=\frac{1}{3}$. The trajectory ends at the top of the energy in the linear region and is described with:

$$\underline{x} = \begin{pmatrix} -\frac{2}{3} - \frac{1}{3}e^{-\frac{1}{2}t} \\ -\frac{2}{3} + \frac{1}{3}e^{-\frac{1}{2}t} \end{pmatrix} \tag{57}$$

In a similar way the trajectory through $(-\frac{1}{3}, -1)$ can be found: K=0, $C_2=-\frac{1}{3}$. As a result the trajectory is described with:

$$\underline{x} = \begin{pmatrix} -\frac{2}{3} + \frac{1}{3}e^{-\frac{1}{2}t} \\ -\frac{2}{3} - \frac{1}{3}e^{-\frac{1}{2}t} \end{pmatrix} \tag{58}$$

Notice that the 'ridge' of the mountain of energy is a straight line through $(-1, -\frac{1}{3})$ and $(-\frac{1}{3}, -1)$ and could have been found too by substituting 'any' other value for x_1 or x_2 when trying to find the top 'a' on the edges I and II respectively! (Equations 57 and 58)

9.3 The BOA in Partially Saturated regions

To find the BOA (this particular trajectory) in the partially saturated regions a trajectory has to be found that runs through $(-1, -\frac{1}{3})$ in region {4} and through $(-\frac{1}{3}, -1)$ in region {8}. Considering region {8} the state equations are given by:

$$\begin{aligned} \dot{x}_1 &= \frac{x_1}{2} \\ \dot{x}_2 &= -x_2 - x_1 + 1 \end{aligned} \tag{59}$$

These equations can be solved to find the trajectories in a similar way as was done for the linear region. In this case it's even simpler; first solve the ODE containing only x_1. Substituting the result in the second ODE and solving this one as well gives:

$$\begin{aligned} x_1 &= C_1 e^{\frac{1}{2}t} \\ x_2 &= \tfrac{2}{3} C_1 e^{\frac{1}{2}t} - \tfrac{1}{2} + C_3 e^{-t} \end{aligned} \tag{60}$$

With some restrictions, 't' can be written as a function of x_1. Substitution of the expression found for 't' into the second equation then gives: $x_2 = \frac{2}{3}x_1 - \frac{1}{2} + \frac{C_3}{\left(\frac{x_1}{C_1}\right)^2} = \frac{2}{3}x_1 - \frac{1}{2} + \frac{K}{(x_1)^2}$. The trajectory through $(-\frac{1}{3}, -1)$ reveals that $K = -\frac{5}{162}$. Thus the BOA in region {8} is given by (see Figure 47):

$$x_2 = \tfrac{2}{3}x_1 - \tfrac{1}{2} - \frac{5}{162(x_1)^2} \tag{61}$$

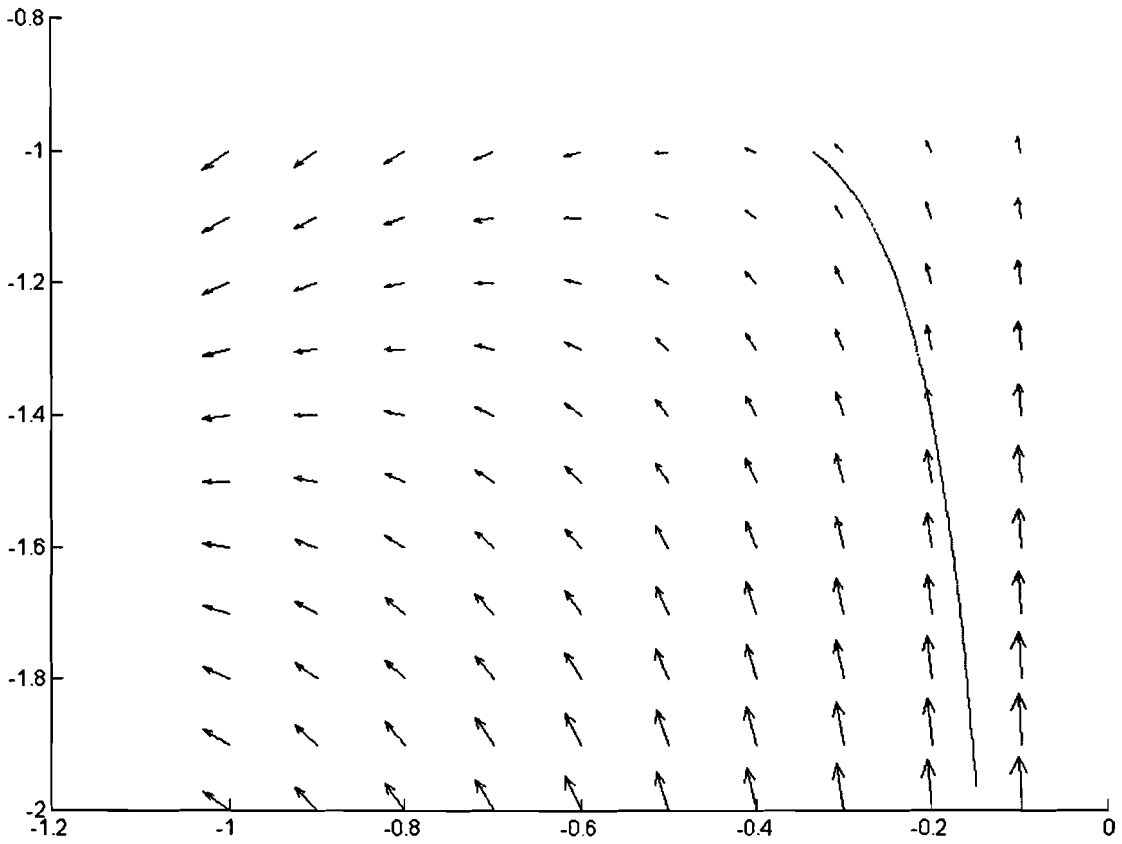

Figure 47 The trajectory and the gradient in partially saturated region

In general this substitution is not always possible and the trajectory can only be given as an explicit function of time. As can be seen the BOA ends in $x_2=-\infty$ for $t\rightarrow-\infty$. The time goes to $-\infty$ and is due to the fact that the gradient is observed which leads to the opposite direction of the actual trajectory (assuming $-\text{grad}(E(x_1,x_2))$ and the state equations are equal). Following the trajectory can thus be done by retracing the gradient. (Following the gradient 'back in time'). Should the trajectory have ended on the edge of the region, then the state equation for the corresponding neighbouring region must be solved and again the trajectory must be continued to infinity.

It is not possible for a BOA to enter (or leave) a fully saturated region that contains a stable equilibrium point. This is true since Zou and Nossek have shown that if there's an equilibrium point in a saturation region, then the whole saturation region belongs to the basin of attraction of that equilibrium point [8]. If the BOA entered such a saturated region then this would mean that at least a part of this region belongs to another basin of attraction and this is a contradiction. Moreover, from this fact it can be concluded that every BOA enters the linear region. Hypothetically this could be only a single point.

When the border between region {7} and {8} is observed, one can find another extreme in the work-function. This must be a phantom-peak since this trajectory would enter a saturated region with a stable equilibrium point. Moreover, it is not connected with the BOA that was found earlier and therefore will not eventually reach the maximum that was found in the linear region. This conclusion is easily made since a two-dimensional state space is observed. In general these phantom peaks cannot be detected so easily, so every peak must be subjected to further study, that is, the trajectory through every peak must be followed. If it does not eventually reach a 'top' then this trajectory is not a BOA and as a result the corresponding peak must be a phantom peak.

10 Finding the BOA

For the two-dimensional case with symmetrical templates, time-independent template parameters and assuming that the trajectory always follows the steepest descent along the energy function in the linear region (which is true for positive definite matrices), the method as described in previous paragraphs appears to be functioning and a scheme can be made for the methodology to find the BOA.

1) Find the work-function along a certain direction on the edge of the linear region. (Changing only one state variable at a time)

2) Find the extreme on this work-function

3) Find the function that describes the extreme as a function of other state variables

4) Repeat step 1-3 for other edges of the linear region

5) Find the general solutions of the state-equations (which describe the trajectories)

6) Find the (set of) solutions for the constants in order to find a specific (set of) trajectory (or trajectories) that go through the extremes that were found

7) Only trajectories that are connected and eventually reach the 'top' are valid trajectories

Ad.3) This is the same as assuming that x_1=constant with $x_1 \in [-1,+1]$ when studying edge I.

Ad.7) As was the case with the phantom-peak on the border between regions {7} and {8}.

If a function can be found that represents a correct energy function then this scheme can be simplified significantly. The maximum of the energy function on the borders of the regions must be found. Solving the state equations and finding the trajectories that go through these extremes then results in a description for the BOA. Even so, it must be verified if every trajectory reaches the absolute top of the energy function. If this is not the case then the ridge that is found describes a local ridge and is not a part of the BOA.

The method as describe above is used on a general 2-cell CNN in Appendix D .

If for example this method is used on a three-dimensional CNN some more work is involved. Assume:

$$\begin{aligned}\dot{x}_1 &= -x_1 + 2y_1 + y_2 + 1\\ \dot{x}_2 &= -x_2 + y_1 + 2y_2 + y_3 + 1\\ \dot{x}_3 &= -x_3 + y_2 + 2y_3 + 1\end{aligned} \tag{62}$$

then four stable equilibrium point in saturated regions can be found: E_1=(4,5,4), E_2=(-2,-3,-2), E_3=(-2,-1,2) and E_4=(2,-1,-2). (Which has been verified experimentally.) In the linear region it can be found that:

$$A=\begin{pmatrix}1 & 1 & 0\\ 1 & 1 & 1\\ 0 & 1 & 1\end{pmatrix} \quad \text{and} \quad \begin{cases}\lambda_1 = 1\\ \lambda_2 = 1+\sqrt{2}\\ \lambda_3 = 1-\sqrt{2}\end{cases} \quad Y^{-1} = \frac{1}{4}\begin{pmatrix}2 & 0 & -2\\ 1 & \sqrt{2} & 1\\ 1 & -\sqrt{2} & 1\end{pmatrix} \tag{63}$$

and thus:

$$\begin{aligned}x_1 &= C_1 e^t - \frac{\left(\frac{1}{2}+\frac{\sqrt{2}}{4}\right)}{1+\sqrt{2}} + C_2 e^{(1+\sqrt{2})t} - \frac{\left(\frac{1}{2}-\frac{\sqrt{2}}{4}\right)}{1-\sqrt{2}} + C_3 e^{(1-\sqrt{2})t}\\ x_2 &= \sqrt{2}C_2 e^{(1+\sqrt{2})t} - \sqrt{2}C_3 e^{(1-\sqrt{2})t} - 1\\ x_3 &= -C_1 e^t - \frac{\left(\frac{1}{2}+\frac{\sqrt{2}}{4}\right)}{1+\sqrt{2}} + C_2 e^{(1+\sqrt{2})t} - \frac{\left(\frac{1}{2}-\frac{\sqrt{2}}{4}\right)}{1-\sqrt{2}} + C_3 e^{(1-\sqrt{2})t}\end{aligned} \tag{64}$$

It can be found that the extremes of the work-function are at: (-1,-1,1), (-1,$\frac{1}{3}$,-1) and (1,-1,-1). The set of extremes of the work-function will always be a linear function of the other state variables. If:

$$\begin{aligned}\underline{F} &= \dot{x}_1 + \dot{x}_2 + \dot{x}_3 + \ldots + \dot{x}_n\\ &= F_1 \cdot \underline{e}_1 + F_2 \cdot \underline{e}_2 + \ldots + F_n \cdot \underline{e}_n + C\end{aligned} \tag{65}$$

then:

$$\begin{aligned}W = \int_{-1}^{a} F \cdot dx_k &= \left[\frac{\alpha}{2}(x_k)^2 + x_k \sum_{\substack{p=1..n\\ p\neq k}} \beta_p x_p + C x_k\right]_{-1}^{a}\\ &= \left[\frac{\alpha}{2}a^2 + a\sum_{\substack{p=1..n\\ p\neq k}} \beta_p x_p + Ca\right] - \left[\frac{\alpha}{2} + \sum_{\substack{p=1..n\\ p\neq k}} \beta_p x_p + C\right]\end{aligned}$$

And:

$$\begin{aligned}\frac{dW}{da} &= \alpha a + \sum_{\substack{p=1..n\\ p\neq k}} \beta_p x_p + C\\ \rightarrow a &= -\frac{\sum_{\substack{p=1..n\\ p\neq k}} \beta_p x_p + C}{\alpha}\end{aligned}$$

So every extreme in the direction of x_p can be expressed as a function of the other state variables x_p ($p \neq k$). For $x_2=-1$ we can find that: $\underline{x} = \begin{pmatrix} \alpha \\ -1 \\ -\alpha \end{pmatrix}$ for $-1 \leq \alpha \leq 1$; the line on the border where all the trajectories will run through that are part of the BOA. Thus the trajectories through this line (assuming t=0) are given by:

$$\underline{x} = \begin{pmatrix} \alpha e^t \\ -1 \\ -\alpha e^t \end{pmatrix} \tag{66}$$

It is easily verified that this is a single line and does not describe a (hyper-) plane. This result is due to the fact that the top of the energy function lies exactly on the border of the linear region. This may be overcome by observing the plane $x_2=-\beta$, with $\beta>-1$ and should be more closely looked at in future studies.

10.1 The BOA with FR-CNN's

To find the basin of attraction for CNN's that are based on the full-range principle will be less complicated, because there is only one region to be studied; the linear region. Every other region is projected onto a certain boundary of the linear region. In the case of saturated regions this boundary reduces to a single point. See Figure 48.

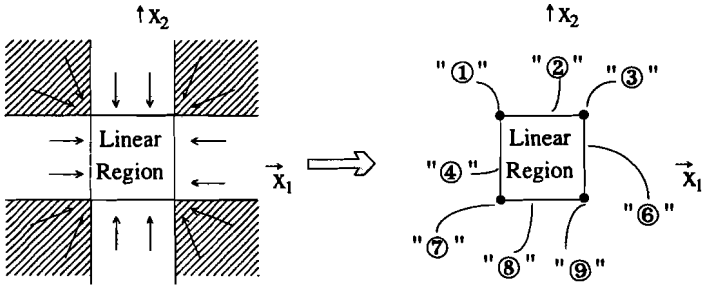

Figure 48 Projection of other regions onto the borders of the linear region

This point however does not necessarily contain a stable equilibrium, but it appears as being stable, because the states cannot become larger than unity. The same effect may appear at other corners, even though the original saturated regions may not have contained a stable equilibrium point. See Figure 49. This can be caused for example by a

gradient in the energy function that 'guides' the trajectory towards region {8} or region {9} which it cannot enter, whereas with regular CNN's the trajectory may have been able to leave region {9} for $x_1>1$. The systems will remain at (1,-1) due to the gradient in the energy function and the saturation function even though at region {9} there may not have been an equilibrium point.

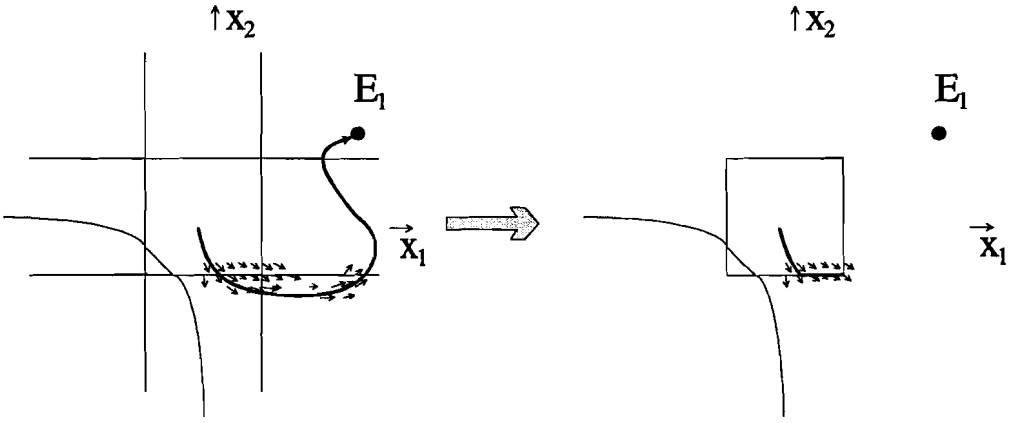

Figure 49 Introduction of stable equilibrium points

The introduction of such an equilibrium point may alter the overall behaviour of a FR-CNN compared to the behaviour of a regular CNN. This may cause unwanted effects and should be more closely looked at in further studies. Thus, although it did not appear so with the example of CCD for which a Matlab program was written (see paragraph 3.3), the FR-CNN may display quite a different behaviour from what can be expected when it uses templates that give a certain desired result with regular CNN's. Whether the introduction of new equilibrium points is possible and what the effects would be should be more closely looked at in future studies.

11 Conclusions and recommendations

First of all, it was shown that the Full-range model as proposed by Rodriguez-Vázquez can be applied, but that the implementation he suggests does not correspond to this Full-range model. The schematic as given by P. Bruin however does implement the Full-range model and is a correct circuit for a cell in a Full-range Cellular Neural Network (FR-CNN).

It is seen that if Level 47 HSPICE parameters are used, the simple square-law formulas no longer accurately describe the behaviour of the transistor and modified parameters have to be found experimentally.

If a cell of a FR-CNN is implemented using only one current mirror and 19 multipliers connected in parallel as suggested, the output impedance of the system is reduced significantly. This causes the cell to show an unexpected behaviour. It was seen that if the output impedance is increased, the proposed cell displays a proper behaviour. This is verified with DC- and transient simulations which were done using the template parameters needed to perform CCD.

In future studies, other operations than CCD should be more closely looked at when the proposed cell structure is used. Also the characteristics of the active diodes to clamp the state voltage to certain pre-defined levels may be improved. The output impedance may be increased even more while the chip area that is needed for VLSI implementation is reduced and the maximum current of 95μA can still be supplied. This will increase the speed with which the CNN operates.

With respect to the boundary of the basin of attraction, it is shown that the BOA can be found in a 2-cell CNN if some restrictions are assumed and if a sort of force is introduced. This is done since it is shown that the used Lyapunov energy function no longer represents a proper energy function. This energy function should describe the behaviour of the cells in every region in state space.

Difficulties arise when the BOA is searched for in CNN's consisting of more than two cells. Although these difficulties may be due to the definition of the force, the method to find the BOA can still be used if a proper energy function is found. A new energy

function that describes the behaviour of the cells in every region in state space should be introduced.

Also, the behaviour of Full-range CNN's should be compared to the behaviour of regular CNN's since it has become clear that undesired stable equilibrium points may be introduced together with the FR-model. Although this does not appear in the examples that were used, other examples may be found where new stable equilibrium points are introduced and should be searched for in future studies.

Acknowledgements

I'd like to thank my coach Hans Hegt for his technical and moral support. He treated me as an equal and gave me the idea that he was as eager 'to tackle this problem' as I was. I'd like to thank my other coach Domine Leenaerts too for the opportunity to have 'another bite of theory' and have me re-experiencing the feelings I had with my first project.

Also I'm much obliged to my friends for moral backup the past few difficult weeks.

Knowing that there were some difficult times ahead, my parents tried to help me as much as possible whereas actually I should have helped them instead. I am very grateful for such wonderful parents and friends. They always remind me of a Dutch phrase: "De boog kan niet altijd gespannen blijven." which has proven quite useful at times!

References

[1] J.A.Hegt, "Neurale Netwerken", department of electrical Engineering, Electronic Circuit Design Group, Eindhoven University of Technology 1994, syllabus.

[2] L.O.Chua, L.Yang, "Cellular Neural Networks: Theory", IEEE Transactions on Circuits and Systems. Vol.35. No.10. October 1988, p.1257-1272

[3] A. Rodriguez-Vázquez et. al. "Current-mode Techniques for the implementation of continuous- and discrete-time cellular neural networks" IEEE Transactions on Circuits and Systems-II: Analogue and Digital processing. Vol.40. No.3, March 1993, p.132-146

[4] P.P.F.M.Bruin, "Electronics for cellular neural networks" , Eindhoven, Stan Ackermans Instituut-Ill. 1993, ISBN 90-5282-612-9

[5] J.A.E.P. van Engelen, "Implementation of an analogue programmable cellular neural network", department of Electrical Engineering, Electronic Circuit Design Group, Thesis, 1995

[6] Y.L.C. de Jong, "Cellulaire neurale netwerken. Een inleidend onderzoek naar werking, toepassingen en implementaties" , department of Electrical Engineering, Electronic Circuit Design Group, Eindhoven University of Technology, 1993

[7] "HSPICE user's manual-software for IC-design" Meta-Software, Inc. Version96.1, February 1996, p.16-157;16-159

[8] F.Zou, J.A.Nossek, "Bifurcation and chaos in cellular neural networks", IEEE Transactions on Circuits and Systems-I: Fundamental Theory and Applications. Vol.40, No.3, March 1993, p.166-173

[9] J.H.Li et al., "Analysis and synthesis of a class of neural networks: linear systems operating on a closed hypercube", IEEE Transactions on Circuits and Systems, Vol.36, November 1989, p.1405-1422

[10] A.N.Michel et al., "Analysis and synthesis techniques for Hopfield type synchronous discrete time neural networks with application to associative memory", IEEE Transactions on Circuits and Systems, Vol.37, November 1990, p.1356-1366

[11] D.Liu, A.N.Michel, "Dynamical systems with saturation non-linearities", Ed. by M. Thoma, Springer-Verlag 1994, ISBN 3-540-19888-1

[12] E.Kreizig, "Advanced engineering mathematics" 6th ed., John Wiley & Sons, 1988, ISBN 0-471-85824-2

Appendix A Ringing caused by active diode

Drained current (μA)	V^+	V^-	V_{end}
2	1.298	1.288	1.292
5	1.306	1.283	1.291
10	1.312	1.277	1.293
20	1.325	1.275	1.298
30	1.339	1.280	1.295
40	1.350	1.285	1.294
50	1.362	1.288	1.294
60	1.374	1.292	1.295
70	1.385	1.295	1.295
80	1.396	--	1.296
95	1.412	--	1.296

Ringing depending on drained current

Ringing shown by output voltage across state capacitor

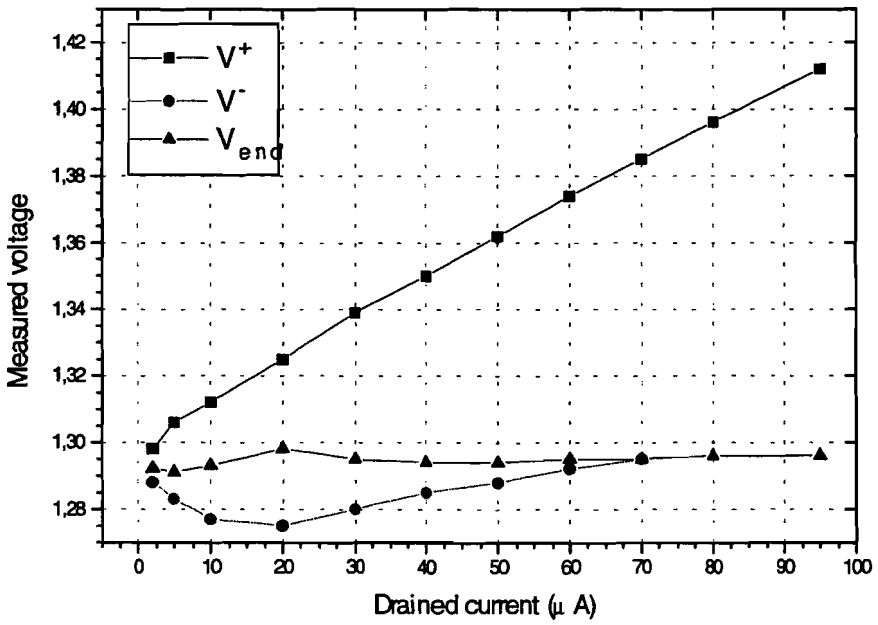

Appendix B HSPICE file :CNNrow6.sp

```
CNNrow6.sp 'CNN - one row of six cells'

*-----------------------------------------------
.subckt multipl Vdd Vin Vw 3 4
M1    2 Vin  Vdd  Vdd PMOSr  1.1u 2.1u
M2    3 Vw   2    Vdd PMOSr  4.2u 1.6u
M3    4 5    2    Vdd PMOSr  4.2u 1.6u
Vwref  5 0 0.95V
.ends

*-----------------------------------------------

.subckt cell Vdd Vin1 Vin2 Vout Vwlft Vwlftc Vwrgt Vwrgtc

* Transistors
M4    3   3 0    0 NMOSr  11.9u 0.8u
M5    4   3 0    0 NMOSr  11.9u 0.8u
Mcl1  6   14  Vdd  Vdd PMOSr  2.6u 0.8u
Mcl2  6   4 0    0 NMOSr  2.6u 1.0u
Mcl3  Vdd  6 4    0 NMOSr  1.1u 0.8u
Mls1  Vout 14 Vdd  Vdd PMOSr  1.1u 1.9u
Mls2  0   4  Vout Vdd PMOSr  1.8u 0.8u
Mch1  9   12  Vdd  Vdd PMOSr  1.7u 6.2u
Mch2  9   4 10   0 NMOSr  5.6u 1.6u
Mch3  7   12  Vdd  Vdd PMOSr  1.7u 6.2u
Mch4  7   13  10   0 NMOSr  5.6u 1.6u
Mch5  10  11  0    0 NMOSr  2.6u 1.6u
Mch6  4   7 0    0 NMOSr  1.1u 0.8u

* Capacitor
C1     4 5  0.7pF *IC=1.3V
R1     5 0  0.1

* Voltage nodes
Vwref   11 0 0.95V
Vbias   14 0 2.2V
VMch1&3  12 0 1.5V
VMch4   13 0 1.3V
* ----------
VAcc    vacc  0  0.6638V
Vnacc   vnacc 0  1.3000V
Vin0    vin0  0  2.0762V
Vw0     vw0   0  0.9666V

* Multipliers
Xacc   Vdd Vout vacc  3 4 multipl
Xaccc  Vdd Vin0 vnacc  3 4 multipl
Xacc1  Vdd Vout vacc  3 4 multipl
Xaccc1  Vdd Vin0 vnacc  3 4 multipl
Xts9   Vdd vin0 vw0   3 4 multipl
Xts10  Vdd vin0 vw0   3 4 multipl
Xleft  Vdd Vin1 vwlft  3 4 multipl
```

```
Xleftc  Vdd vin0 vwlftc 3 4 multipl
Xright  Vdd Vin2 vwrgt  3 4 multipl
Xrightc Vdd vin0 vwrgtc 3 4 multipl
Xts11   Vdd vin0 vw0    3 4 multipl
Xts12   Vdd vin0 vw0    3 4 multipl
Xts13   Vdd vin0 vw0    3 4 multipl
Xts14   Vdd vin0 vw0    3 4 multipl
Xts15   Vdd vin0 vw0    3 4 multipl
Xts16   Vdd vin0 vw0    3 4 multipl
Xts17   Vdd vin0 vw0    3 4 multipl
Xts18   Vdd vin0 vw0    3 4 multipl
Xts19   Vdd vin0 vw0    3 4 multipl


.ends
*-----------------------------------------------

.subckt EcellL Vdd Vin1 Vin2 Vout Vwlft Vwlftc Vwrgt Vwrgtc

* Transistors
M4     3    3  0     0 NMOSr  11.9u 0.8u
M5     4    3  0     0 NMOSr  11.9u 0.8u
Mcl1   6    14 Vdd   Vdd PMOSr  2.6u 0.8u
Mcl2   6    4  0     0 NMOSr  2.6u 1.0u
Mcl3   Vdd  6  4     0 NMOSr  1.1u 0.8u
Mls1   Vout 14 Vdd   Vdd PMOSr  1.1u 1.9u
Mls2   0    4  Vout  Vdd PMOSr  1.8u 0.8u
Mch1   9    12 Vdd   Vdd PMOSr  1.7u 6.2u
Mch2   9    4  10    0 NMOSr  5.6u 1.6u
Mch3   7    12 Vdd   Vdd PMOSr  1.7u 6.2u
Mch4   7    13 10    0 NMOSr  5.6u 1.6u
Mch5   10   11 0     0 NMOSr  2.6u 1.6u
Mch6   4    7  0     0 NMOSr  1.1u 0.8u

* Capacitor
C1     4 5  0.7pF *IC=1.3V
R1     5 0  0.1

* Voltage nodes
Vwref    11 0 0.95V
Vbias    14 0 2.2V
VMch1&3  12 0 1.5V
VMch4    13 0 1.3V
* ----------
VAcc     vacc  0  0.6638V
Vnacc    vnacc 0  1.3000V
Vin0     vin0  0  2.0762V
Vw0      vw0   0  0.9666V

* Multipliers
Xacc   Vdd Vout vacc   3 4 multipl
Xaccc  Vdd Vin0 vnacc  3 4 multipl
Xacc1  Vdd Vout vacc   3 4 multipl
Xaccc1 Vdd Vin0 vnacc  3 4 multipl
Xacc2  Vdd Vout vacc   3 4 multipl
Xaccc2 Vdd Vin0 vnacc  3 4 multipl
```

```
Xleft  Vdd Vin0 vw0   3 4 multipl
Xleftc Vdd vin0 vw0   3 4 multipl
Xright Vdd Vin2 vwrgt 3 4 multipl
Xrightc Vdd vin0 vwrgtc 3 4 multipl
Xts11  Vdd vin0 vw0   3 4 multipl
Xts12  Vdd vin0 vw0   3 4 multipl
Xts13  Vdd vin0 vw0   3 4 multipl
Xts14  Vdd vin0 vw0   3 4 multipl
Xts15  Vdd vin0 vw0   3 4 multipl
Xts16  Vdd vin0 vw0   3 4 multipl
Xts17  Vdd vin0 vw0   3 4 multipl
Xts18  Vdd vin0 vw0   3 4 multipl
Xts19  Vdd vin0 vw0   3 4 multipl


.ends
*---------------------------------------------------

.subckt EcellR Vdd Vin1 Vin2 Vout Vwlft Vwlftc Vwrgt Vwrgtc

* Transistors
M4    3   3 0    0 NMOSr  11.9u 0.8u
M5    4   3 0    0 NMOSr  11.9u 0.8u
Mcl1  6   14  Vdd  Vdd PMOSr  2.6u 0.8u
Mcl2  6   4 0    0 NMOSr  2.6u 1.0u
Mcl3  Vdd  6 4    0 NMOSr  1.1u 0.8u
Mls1  Vout 14  Vdd  Vdd PMOSr  1.1u 1.9u
Mls2  0   4  Vout Vdd PMOSr  1.8u 0.8u
Mch1  9   12  Vdd  Vdd PMOSr  1.7u 6.2u
Mch2  9   4 10   0 NMOSr  5.6u 1.6u
Mch3  7   12  Vdd  Vdd PMOSr  1.7u 6.2u
Mch4  7   13 10   0 NMOSr  5.6u 1.6u
Mch5  10  11 0    0 NMOSr  2.6u 1.6u
Mch6  4   7 0    0 NMOSr  1.1u 0.8u

* Capacitor
C1     4 5  0.7pF *IC=1.3V
R1     5 0  0.1

* Voltage nodes
Vwref   11 0 0.95V
Vbias   14 0 2.2V
VMch1&3  12 0 1.5V
VMch4   13 0 1.3V
* ----------
VAcc    vacc 0  0.6638V
Vnacc   vnacc 0  1.3000V
Vin0    vin0 0  2.0762V
Vw0     vw0  0  0.9666V

* Multipliers
Xacc   Vdd Vout vacc  3 4 multipl
Xaccc  Vdd Vin0 vnacc  3 4 multipl
Xacc1  Vdd Vout vacc  3 4 multipl
Xaccc1  Vdd Vin0 vnacc  3 4 multipl
Xacc2  Vdd Vout vacc  3 4 multipl
```

```
Xaccc2  Vdd Vin0 vnacc  3 4 multipl
Xleft   Vdd Vin1 vwlft  3 4 multipl
Xleftc  Vdd vin0 vwlftc 3 4 multipl
Xright  Vdd Vin0 vw0    3 4 multipl
Xrightc Vdd vin0 vw0    3 4 multipl
Xts11   Vdd vin0 vw0    3 4 multipl
Xts12   Vdd vin0 vw0    3 4 multipl
Xts13   Vdd vin0 vw0    3 4 multipl
Xts14   Vdd vin0 vw0    3 4 multipl
Xts15   Vdd vin0 vw0    3 4 multipl
Xts16   Vdd vin0 vw0    3 4 multipl
Xts17   Vdd vin0 vw0    3 4 multipl
Xts18   Vdd vin0 vw0    3 4 multipl
Xts19   Vdd vin0 vw0    3 4 multipl


.ends
*--------------------------------------------------
*--------------------------------------------------

.tran 10ns 1500ns
*.op 50ns

.IC V(X1.4)=0.9V
+  V(X2.4)=1.3V
+  V(X3.4)=1.3V
+  V(X4.4)=1.3V
+  V(X5.4)=1.3V
+  V(X6.4)=0.9V


Vdd      1  0 3.3V
VwNill   40 0 0.9667V
Vwlft    41 0 0.7979V
Vwlftc   42 0 1.1429V
Vwrgt    43 0 1.1429V
Vwrgtc   44 0 0.7979V
VinNill  45 0 2.0762V


X1 1 45 u2 u1 40 40 43 44 EcellL
X2 1 u1 u3 u2 41 42 43 44 cell
X3 1 u2 u4 u3 41 42 43 44 cell
X4 1 u3 u5 u4 41 42 43 44 cell
X5 1 u4 u6 u5 41 42 43 44 cell
X6 1 u5 45 u6 41 42 40 40 EcellR

.print V(u1) V(u2) V(u3) V(u4) V(u5) V(u6)
+  V(X1.4)
+  V(X2.4)
+  V(X3.4)
+  V(X4.4)
+  V(X5.4)
+  V(X6.4)
+ I3(X1.Xacc.M1) V(X1.Xacc.2) V(X1.Xacc.3) V(X1.Xacc.4)
```

```
.option WL POST OFF NOMOD ABSMOS=1E-12 RELVDC=0.001 RELMOS=0.001
+ LVLTIM=3 DVDT=2 ABSVAR=1E-7 PIVOT=13
+ RELTOL=1E-7 method=gear *VNTOL=1E-14 *RMAX=0.01
.temp 27


.MODEL NMOSR NMOS LEVEL=47
+VTHO=0.6167061        K1=0.5992536        K2=9.681673E-3
+K3=0.0664731      K3B=0.0848494      W0=2.011142E-6
+NLX=1.016643E-7   DVT0=4.0537809     DVT1=0.7140707
+DVT2=-0.015361        DL=3E-8             DW=2.301932E-8
+UA=6.124312E-10   UB=1.932798E-18    UC=0.0125756
+VSAT=8.922874E6   A0=0.6067592       KETA=-0.0166963
+A1=0              A2=1           RDS0=2.3
+RDSW=765.8949964  VOFF=-0.0335402    NFACTOR=1.64108
+CDSC=2E-5         CDSCB=9.1684E-5         ETA0=0.0104031
+ETAB=3.090849E-3  DSUB=0.0578341     PCLM=1.5982969
+PDIBL1=0.1035115  PDIBL2=1.1703E-3   DROUT=0.5158942
+PSCBE1=1.30884E8  PSCBE2=7.363849E-8 PVAG=0.3064459
+UTE=-1.5856242    KT1=-0.1102432     KT1L=-1.2E-9
+KT2=0.0226957     UA1=1.116809E-10   UB=0
+UC1=-0.06         AT=1.022222E4      TOX=1.03E-8
+XJ=2E-7       NPEAK=1.1E17       NSUB=4E16
+SUBTHMOD=3       SATMOD=2           BULKMOD=1
+XPART=1       XT=1.55E-7      VBM=-5
+U0=517.8468925   ETA=0.3            VGHIGH=0.15
+VGLOW=-0.15      CIT=0              JS=0
+RSH=0            CGDO=1.312E-10     CGSO=1.312E-10
+CGBO=3.28E-10    CJ=7.5E-4          PB=0.74
+MJ=0.35       CJSW=3.4E-10

.MODEL PMOSR PMOS LEVEL=47
+VTHO=-0.5406341   K1=0.6124669       K2=0.0178682
+K3=21.4923586     K3B=-8.6159594     W0=8.875616E-6
+NLX=1.892983E-7   DVT0=3.4224992     DVT1=0.6409558
+DVT2=0.0114412        DL=3.455666E-8      DW=0
+UA=1.386541E-9        UB=8.471541E-19     UC=-0.0276702
+VSAT=6.210514E6   A0=3.9             KETA=-0.0835983
+A1=0.1772758      A2=7.15954E-3      RDS0=2.7
+RDSW=1.991187E3   VOFF=-0.0835342    NFACTOR=1.420078
+CDSC=2E-5         CDSCB=1.889443E-3  ETA0=0.0799679
+ETAB=-0.0699861   DSUB=0.05602321        PCLM=2.7224552
+PDIBL1=0.3863554  PDIBL2=1.621787E-3  DROUT=0.6291645
+PSCBE1=1E8        PSCBE2=1.001E-10    PVAG=-0.2990312
+UTE=-1.253412     KT1=0.113123       KT1L=-1.00423E-9
+KT2=0.0226957     UA1=1.11689E-10         UB=0
+UC1=-0.0556       AT=5.553421E-10    TOX=1.03E-8
+XJ=2E-7       NPEAK=1.1E17       NSUB=4E16
+SUBTHMOD=3       SATMOD=2           BULKMOD=2
+XPART=1       XT=1.55E-7      VBM=-5
+U0=130.5451767   ETA=0.3            VGHIGH=0.15
+VGLOW=-0.15      CIT=0              JS=0
+RSH=0            CGDO=1.312E-10     CGSO=1.312E-10
+CGBO=3.28E-10    CJ=7.9E-4          PB=0.83
+MJ=0.39       CJSW=4.2E-10
```

```
.MODEL NMOSF NMOS LEVEL=47
+VTHO=0.5667061          K1=0.5992536          K2=9.681673E-3
+K3=0.0664731          K3B=0.0848494          W0=2.011142E-6
+NLX=1.016643E-7     DVT0=4.0537809       DVT1=0.7140707
+DVT2=-0.015361          DL=7E-8               DW=-1.698068E-8
+UA=6.124312E-10     UB=1.932798E-18      UC=0.0125756
+VSAT=8.282874E6     A0=0.6067592         KETA=-0.0166963
+A1=0                A2=1                 RDS0=2.3
+RDSW=765.8949964    VOFF=-0.0335402      NFACTOR=1.6410763
+CDSC=2E-5           CDSCB=9.1684E-5           ETA0=0.0104031
+ETAB=3.090849E-3    DSUB=0.0578341       PCLM=1.5982969
+PDIBL1=0.1035115    PDIBL2=1.1703E-3     DROUT=0.5158942
+PSCBE1=1.30884E8    PSCBE2=7.363849E-8   PVAG=0.3064459
+UTE=-1.5856242      KT1=-0.1102432       KT1L=-1.2E-9
+KT2=0.0226957       UA1=1.116809E-10     UB=0
+UC1=-0.06           AT=1.022222E4        TOX=0.97E-8
+XJ=2E-7         NPEAK=1.1E17         NSUB=4E16
+SUBTHMOD=3          SATMOD=2             BULKMOD=1
+XPART=1         XT=1.55E-7       VBM=-5
+U0=517.8468925      ETA=0.3              VGHIGH=0.15
+VGLOW=-0.15         CIT=0                JS=0
+RSH=0               CGDO=1.312E-10       CGSO=1.312E-10
+CGBO=3.28E-10       CJ=7.5E-4        PB=0.74
+MJ=0.35         CJSW=3.4E-10         PBSW=0.74
+MSJW=0.29

.MODEL PMOSF PMOS LEVEL=47
+VTHO=-0.4906341     K1=0.6124669         K2=0.0178682
+K3=21.4923586       K3B=-8.6159594       W0=8.875616E-6
+NLX=1.892983E-7     DVT0=3.4224992       DVT1=0.6409558
+DVT2=0.0114412          DL=7.455666E-8        DW=-4E-8
+UA=1.386541E-9           UB=8.471541E-19      UC=-0.0276702
+VSAT=5.390514E6     A0=3.9               KETA=-0.0835983
+A1=0.1772758        A2=7.15954E-3        RDS0=2.7
+RDSW=1.991187E3     VOFF=-0.0835342      NFACTOR=1.420078
+CDSC=2E-5           CDSCB=1.889443E-3    ETA0=0.0799679
+ETAB=-0.0699861     DSUB=0.05602321           PCLM=2.7224552
+PDIBL1=0.3863554    PDIBL2=1.621787E-3   DROUT=0.6291645
+PSCBE1=1E8          PSCBE2=1.001E-10     PVAG=-0.2990312
+UTE=-1.253412       KT1=0.113123         KT1L=-1.00423E-9
+KT2=0.0226957       UA1=1.11689E-10           UB=0
+UC1=-0.0556         AT=5.553421E-10      TOX=0.97E-8
+XJ=2E-7         NPEAK=1.1E17         NSUB=4E16
+SUBTHMOD=3          SATMOD=2             BULKMOD=2
+XPART=1         XT=1.55E-7       VBM=-5
+U0=130.5451767      ETA=0.3              VGHIGH=0.15
+VGLOW=-0.15         CIT=0                JS=0
+RSH=0               CGDO=1.312E-10       CGSO=1.312E-10
+CGBO=3.28E-10       CJ=7.9E-4        PB=0.83
+MJ=0.39         CJSW=4.2E-10         PBSW=0.83
+MSJW=0.35

.MODEL NMOSS NMOS LEVEL=47
+VTHO=0.6667061          K1=0.5992536          K2=9.681673E-3
+K3=0.0664731          K3B=0.0848494          W0=2.011142E-6
```

```
+NLX=1.016643E-7    DVT0=4.0537809      DVT1=0.7140707
+DVT2=-0.015361          DL=-1E-8       DW=6.301932E-8
+UA=6.124312E-10    UB=1.932798E-18     UC=0.0125756
+VSAT=9.084287E6    A0=0.6067592        KETA=-0.0166963
+A1=0               A2=1           RDS0=2.3
+RDSW=765.8949964   VOFF=-0.0335402    NFACTOR=1.6410763
+CDSC=2E-5          CDSCB=9.16839E-5    ETA0=0.0104031
+ETAB=3.090849E-3   DSUB=0.0578341      PCLM=1.5982969
+PDIBL1=0.1035115   PDIBL2=1.170287E-3  DROUT=0.5158942
+PSCBE1=1.30884E8   PSCBE2=7.363849E-8  PVAG=0.3064459
+UTE=-1.5856242     KT1=-0.1102432      KT1L=-1.2E-9
+KT2=0.0226957      UA1=1.116809E-10    UB=0
+UC1=-0.06          AT=1.022222E4       TOX=1.03E-8
+XJ=2E-7       NPEAK=1.1E17        NSUB=4E16
+SUBTHMOD=3       SATMOD=2          BULKMOD=1
+XPART=1       XT=1.55E-7       VBM=-5
+U0=517.8468925     ETA=0.3             VGHIGH=0.15
+VGLOW=-0.15        CIT=0               JS=0
+RSH=0              CGDO=1.312E-10      CGSO=1.312E-10
+CGBO=3.28E-10      CJ=7.5E-4       PB=0.74
+MJ=0.35       CJSW=3.4E-10         PBSW=0.74
+MSJW=0.29


.MODEL PMOSS PMOS LEVEL=47
+VTHO=-0.5906341    K1=0.6124669        K2=0.0178682
+K3=21.4923586      K3B=-8.6159594      W0=8.875616E-6
+NLX=1.892983E-7    DVT0=3.4224992      DVT1=0.6409558
+DVT2=0.0114412          DL=-0.544334E-8      DW=4E-8
+UA=1.386541E-9          UB=8.471541E-19      UC=-0.0276702
+VSAT=6.9450514E6   A0=3.9              KETA=-0.0835983
+A1=0.1972758       A2=7.15954E-3       RDS0=2.7
+RDSW=1.991187E3    VOFF=-0.0835342     NFACTOR=1.4200784
+CDSC=2E-5          CDSCB=1.889443E-3   ETA0=0.0799679
+ETAB=-0.0699861    DSUB=0.05602321          PCLM=2.7224552
+PDIBL1=0.3863554   PDIBL2=1.621787E-3  DROUT=0.6291645
+PSCBE1=1E8         PSCBE2=1.001E-10    PVAG=-0.2990312
+UTE=-1.253412      KT1=0.113123        KT1L=-1.00423E-9
+KT2=0.0226957      UA1=1.11689E-10          UB=0
+UC1=-0.0556        AT=5.553421E-10     TOX=1.03E-8
+XJ=2E-7       NPEAK=1.1E17        NSUB=4E16
+SUBTHMOD=3       SATMOD=2          BULKMOD=2
+XPART=1       XT=1.55E-7       VBM=-5
+U0=130.5451767     ETA=0.3             VGHIGH=0.15
+VGLOW=-0.15        CIT=0               JS=0
+RSH=0              CGDO=1.312E-10      CGSO=1.312E-10
+CGBO=3.28E-10      CJ=7.9E-4       PB=0.83
+MJ=0.39       CJSW=4.2E-10         PBSW=0.83
+MSJW=0.35
.end
```

Appendix C Currents through state capacitor

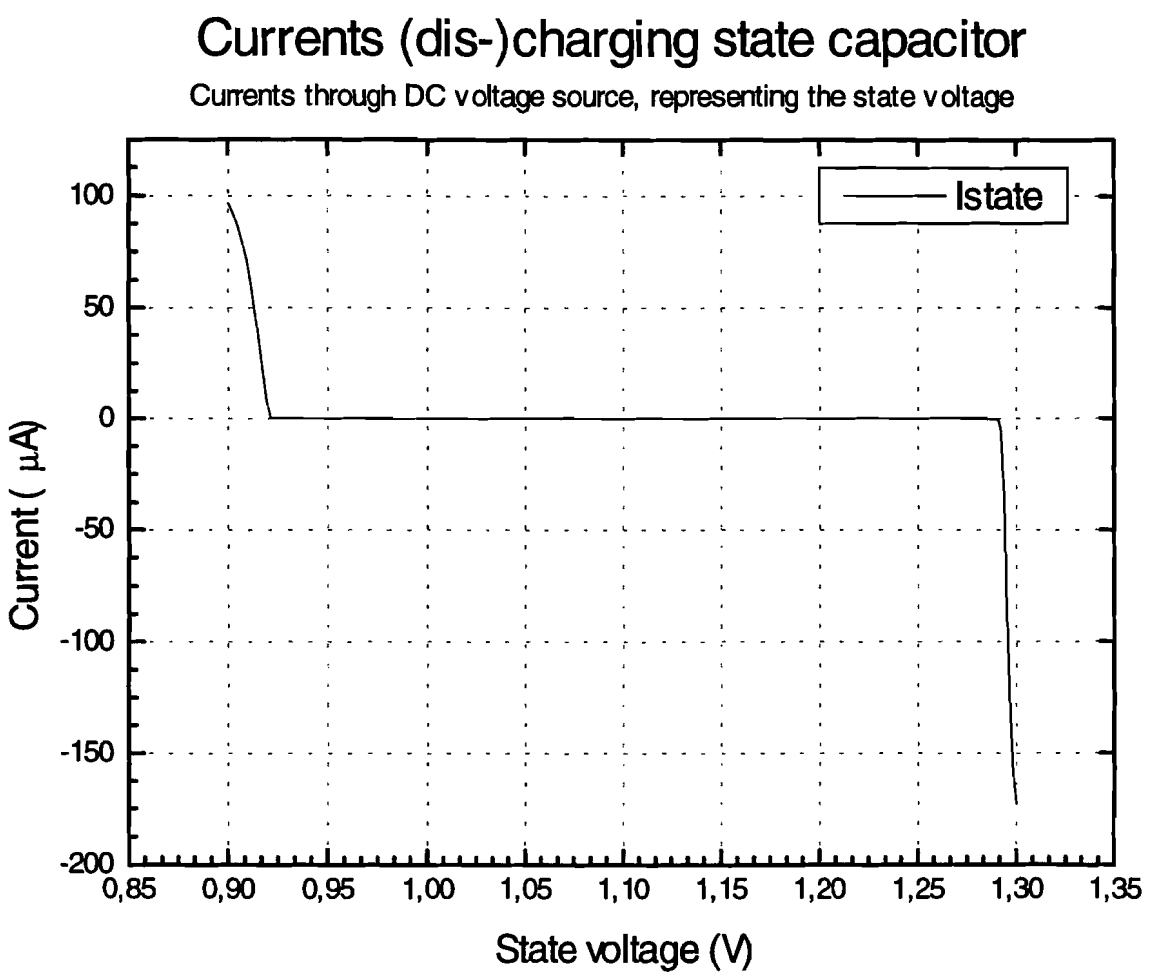

The state capacitor is replaced with a DC-voltage source and the DC-voltage is varied

Appendix D 'BOA of a 2-cell CNN'

The following calculations are only valid for 2-cell CNN's with symmetrical templates and for which the trajectory 'follows the steepest path down the energy-function'.

If for a 2-cell CNN the state equations are given by:

$$\dot{x}_1 = A_1 x_1 + a_1{}^1 y_1 + a_2{}^1 y_2 + B_1$$
$$\dot{x}_2 = A_2 x_2 + a_1{}^2 y_1 + a_2{}^2 y_2 + B_2$$

then for the linear region it can be found that:

$$\dot{x}_1 = A_1 x_1 + a_1{}^1 x_1 + a_2{}^1 x_2 + B_1$$
$$\dot{x}_2 = A_2 x_2 + a_1{}^2 x_1 + a_2{}^2 x_2 + B_2$$

If the force F is defined as:

$$\underline{F} = \dot{x}_1 + \dot{x}_2$$

it is found that:

$$\underline{F} = \underbrace{\left(A_1 + a_1{}^1 + a_1{}^2\right)}_{\alpha} x_1 + \underbrace{\left(a_2{}^1 + A_2 + a_2{}^2\right)}_{\beta} x_2 + \underbrace{\left(B_1 + B_2\right)}_{\gamma}$$

Integration along edges I and III of the linear region then gives (See Figure 45 and Figure 46):

$$W = \int_{-1}^{a} \alpha x_1 + \beta x_2 + \gamma \, dx_2$$

$$= \left[\frac{\beta}{2}(x_2)^2 + (\alpha x_1 + \gamma)x_2\right]_{-1}^{a} = \left(\frac{\beta}{2}a^2 + (\alpha x_1 + \gamma)a\right) - \left(\frac{\beta}{2} - (\alpha x_1 + \gamma)\right)$$

To find the extreme:

$$\frac{dW}{da} = 0$$

$$\beta\ a + (\alpha x_1 + \gamma) = 0$$

$$a = -\frac{(\alpha x_1 + \gamma)}{\beta}$$

Thus, for Edge I and III;

$$a = \frac{A_1 + a_1{}^1 + a_1{}^2 - B_1 - B_2}{a_2{}^1 + A_2 + a_2{}^2} \text{ and } a = -\frac{A_1 + a_1{}^1 + a_1{}^2 + B_1 + B_2}{a_2{}^1 + A_2 + a_2{}^2} \text{ respectively.}$$

Likewise for edge II and IV it is found that:

$$a = \frac{a_2{}^1 + A_2 + a_2{}^2 - B_1 - B_2}{A_1 + a_1{}^1 + a_1{}^2} \text{ and } a = -\frac{a_2{}^1 + A_2 + a_2{}^2 + B_1 + B_2}{A_1 + a_1{}^1 + a_1{}^2} \text{ respectively.}$$

To find the trajectories assume:

$$\dot{\underline{x}} = \underline{F} = \begin{pmatrix} a_1{}^1 + A_1 & a_2{}^1 \\ a_1{}^2 & a_2{}^2 + A_2 \end{pmatrix} \underline{x} + \begin{pmatrix} B_1 \\ B_2 \end{pmatrix} = A\underline{x} + \underline{h}$$

The eigenvalues are found with:

$$\det(A-\lambda I)=0$$

$$\leftrightarrow$$

$$\begin{vmatrix} a_1^{\,1}+A_1-\lambda & a_2^{\,1} \\ a_1^{\,2} & a_2^{\,2}+A_2-\lambda \end{vmatrix}=0$$

So:

$$\left(a_1^{\,1}+A_1-\lambda\right)\left(a_2^{\,2}+A_2-\lambda\right)-a_1^{\,2}a_2^{\,1}=0$$

$$\lambda^2-\left(a_1^{\,1}+A_1+a_2^{\,2}+A_2\right)\lambda+\left(a_1^{\,1}+A_1\right)\left(a_2^{\,2}+A_2\right)-a_1^{\,2}a_2^{\,1}=0$$

and as a result:

$$\lambda_{1,2}=\frac{a_1^{\,1}+A_1+a_2^{\,2}+A_2\pm\sqrt{\left(a_1^{\,1}+A_1+a_2^{\,2}+A_2\right)^2-4\left(a_1^{\,1}+A_1\right)\left(a_2^{\,2}+A_2\right)+4a_1^{\,2}a_2^{\,1}}}{2}$$

If:

$$\underline{Y}_1\Rightarrow x_1\left(a_1^{\,1}+A_1-\lambda_1\right)+a_2^{\,1}x_2=0$$

$$x_2=-\frac{\left(a_1^{\,1}+A_1-\lambda_1\right)}{a_2^{\,1}}$$

then: $\underline{Y}_1=\begin{pmatrix}-1\\ \dfrac{\left(a_1^{\,1}+A_1-\lambda_1\right)}{a_2^{\,1}}\end{pmatrix}$ and likewise: $\underline{Y}_2=\begin{pmatrix}-1\\ \dfrac{\left(a_1^{\,1}+A_1-\lambda_2\right)}{a_2^{\,1}}\end{pmatrix}$

If $Y=\left(\underline{Y}_1\quad\underline{Y}_2\right)$ then:

$$Y=\begin{pmatrix}-1 & -1\\ \dfrac{\left(a_1^{\,1}+A_1-\lambda_1\right)}{a_2^{\,1}} & \dfrac{\left(a_1^{\,1}+A_1-\lambda_2\right)}{a_2^{\,1}}\end{pmatrix}$$

Also:

$$Y^{-1}=\begin{pmatrix}\dfrac{\left(a_1^{\,1}+A_1-\lambda_2\right)}{\lambda_2-\lambda_1} & \dfrac{a_2^{\,1}}{\lambda_2-\lambda_1}\\ \dfrac{\left(a_1^{\,1}+A_1-\lambda_1\right)}{\lambda_1-\lambda_2} & \dfrac{a_2^{\,1}}{\lambda_1-\lambda_2}\end{pmatrix}$$

If $\underline{x}=Y\underline{z}$ then:

$$Y\dot{\underline{z}}=AY\underline{z}+\underline{h}$$

$$\dot{\underline{z}}=Y^{-1}AY\underline{z}+Y^{-1}\underline{h}$$

$$=D\underline{z}+Y^{-1}\underline{h}$$

or: $\dot{\underline{z}}=\begin{pmatrix}\lambda_1 & 0\\ 0 & \lambda_2\end{pmatrix}\begin{pmatrix}z_1\\ z_2\end{pmatrix}+Y^{-1}\begin{pmatrix}B_1\\ B_2\end{pmatrix}$.

In general, if: $\dot{z}=\alpha z+\beta$ then $z=-\dfrac{\beta}{\alpha}+Ce^{\alpha t}$

and as a result:

$$z_1 = \frac{B_1\left(A_1 - \lambda_2 + a_1^1\right) + B_2 a_2^1}{\left(\lambda_1 - \lambda_2\right)\lambda_1} + C_1 e^{\lambda_1 t}$$

$$z_2 = \frac{B_1\left(A_1 - \lambda_1 + a_1^1\right) + B_2 a_2^1}{\left(\lambda_2 - \lambda_1\right)\lambda_2} + C_2 e^{\lambda_2 t}$$

Finally, the trajectories are then described by:

$$x_1 = \frac{B_1\left(A_1 - \lambda_2 + a_1^1\right) + B_2 a_2^1}{\left(\lambda_2 - \lambda_1\right)\lambda_1} - C_1 e^{\lambda_1 t} + \frac{B_1\left(A_1 - \lambda_1 + a_1^1\right) + B_2 a_2^1}{\left(\lambda_2 - \lambda_1\right)\lambda_2} - C_2 e^{\lambda_2 t}$$

$$x_2 = \left(\frac{A_1 - \lambda_1 + a_1^1}{a_2^1}\right)\left(\frac{B_1\left(A_1 - \lambda_2 + a_1^1\right) + B_2 a_2^1}{\left(\lambda_2 - \lambda_1\right)\lambda_1} + C_1 e^{\lambda_1 t}\right) +$$

$$\left(\frac{A_1 - \lambda_2 + a_1^1}{a_2^1}\right)\left(\frac{B_1\left(A_1 - \lambda_1 + a_1^1\right) + B_2 a_2^1}{\left(\lambda_2 - \lambda_1\right)\lambda_2} + C_2 e^{\lambda_2 t}\right)$$